X-732-67-3

55660

DESIGN OF A SINGLE AXIS SIMULATOR FOR SATELLITE CONTROL SYSTEM TESTING AND FOR LOW TORQUE MEASUREMENT

BY

CLARENCE CANTOR
JOHN HRASTAR
JOHN KELLY

JANUARY 1967

GODDARD SPACE FLIGHT CENTER

GREENBELT, MARYLAND

DESIGN OF A SINGLE AXIS SIMULATOR FOR SATELLITE CONTROL SYSTEM TESTING AND FOR LOW TORQUE MEASUREMENT

by

Clarence Cantor

John Hrastar

John Kelly

Stabilization & Control Branch—
Systems Division

January 1967

GODDARD SPACE FLIGHT CENTER
Greenbelt, Maryland

ACKNOWLEDGEMENTS

The authors wish to acknowledge the important contributions to this project by the following Stabilization and Control Branch:

Henry Hoffman	general direction of project
Robert Peterson	design of pneumatic system for the hydrogen microthruster
Kurt Andersen	checkout and design modification of telemetry and command systems
Robert Ballard	lead technician on the development, integration and checkout of the single axis and microthruster tables
Don Rowley	wiring of microthruster table and test consoles
Andrew Muir	preparation of report illustrations

TABLE OF CONTENTS

LIST OF ILLUSTRATIONS

DESIGN OF A SINGLE AXIS SIMULATOR FOR SATELLITE CONTROL SYSTEM TESTING AND FOR LOW TORQUE MEASUREMENT

I. INTRODUCTION

This report describes a single-axis simulator design of the authors, for use in testing satellite control systems and components. Two models of the simulator have been built. The first, called a single-axis table, has a large load capacity which is capable of checking most reaction jet-inertia wheel type of control systems, in a torque-free environment (zero torque mode). This model also incorporates a novel, long period oscillation mode for use in checking electro-magnetic dampers used in gravity gradient controlled satellites. The second model, called a microthruster table, is a smaller version of the first for use in checking microthrusters (10^{-6} to 2×10^{-4} lbs) and microthruster control systems, in a vacuum chamber. In addition to the zero torque mode, this model also has a novel, continuous torque mode for continuous "instantaneous" measurement of torque generated by the microthruster under test.

II. GENERAL DESCRIPTION

The basic configuration of the single axis table is shown schematically in Figure 1. The single-axis table consists of a platform suspended by a cable having a low torsional spring constant. (See Reference 2 for design of the ultra-soft torsional cable.) An electronic autocollimator measures the twist in the cable by sighting on a small mirror on a tube attached to the platform. The signal from this autocollimator is used to control a follow-up servo drive to which the top of the cable is attached. Two different modes of operation can be incorporated in this basic configuration. These are called the zero torque mode and the long period oscillation mode.

A block diagram of table operation in the zero torque or long period oscillation modes is shown in Figure 2. For operation in the zero torque mode the control system or component under test is placed on the platform. The torque generated by this system or component will produce platform rotation θ. The wire will twist through an angle α which is the difference between table motion θ and follow-up drive rotation θ_f. This angular twist α is sensed by the electronic autocollimator via a mirror attached to a rigid tube which in turn is rigidly attached to the platform. The sensor signal produced by this angular twist α is fed to the follow-up drive which rotates the top suspension for the wire so as to reduce wire twist α to zero. The speed of this follow-up response is fast compared to the platform motion θ produced by the system under test. Hence, the wire twist α remains near zero throughout the test. This means that the platform has "zero" external torque applied to it except for the torque generated by the system under test. Thus the control system or component under test can be carefully evaluated by measuring platform motion θ.

In the long period oscillation mode, the wire twist α at any instant is not reduced to zero, but to a value that is a small, precise percentage of the twist that would be experienced with no follow-up motion. This is accomplished by feeding back a signal from a feedback potentiometer that measures follow-up servo rotation. This potentiometer signal is mixed with the autocollimator signal, as shown in Figure 2, so that in equilibrium, a small twist α remains in the wire. For example, if the table were moved 10° from equilibrium, the follow-up drive servo loop could be pre-set so as to automatically follow-up a precise 9.9°. This would leave a 0.1° twist in the cable and hence a small restoring torque on the platform. The effective spring constant in this arrangement is only 1% of the natural spring constant of the wire since the wire is twisted by an amount equal to only 1% of table motion θ, starting from equilibrium. The decrease of the natural spring constant is adjustable up to a factor of about 500, through a pre-set adjustment in the servo loop gain. Thus

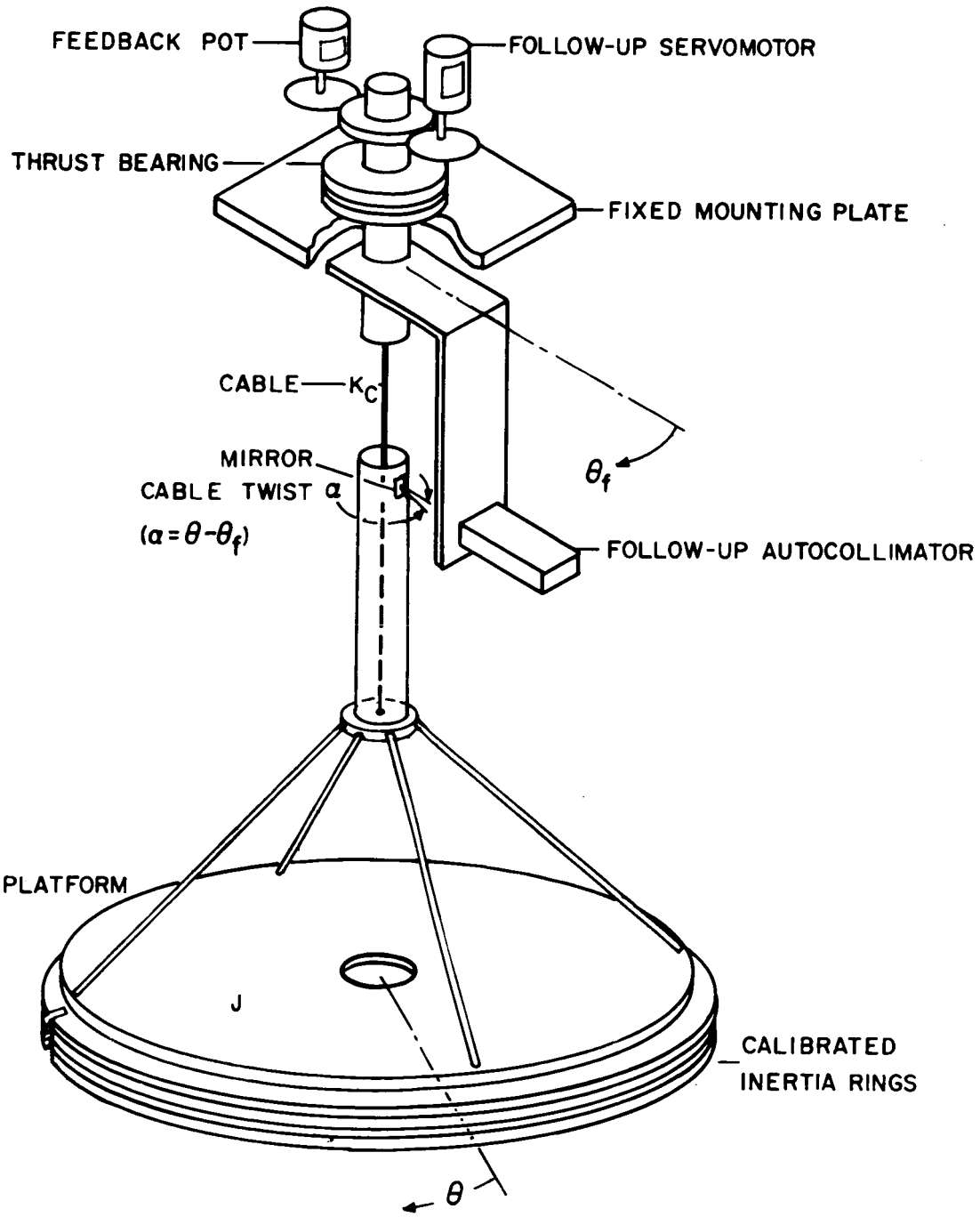

Figure 1. Single Axis Table

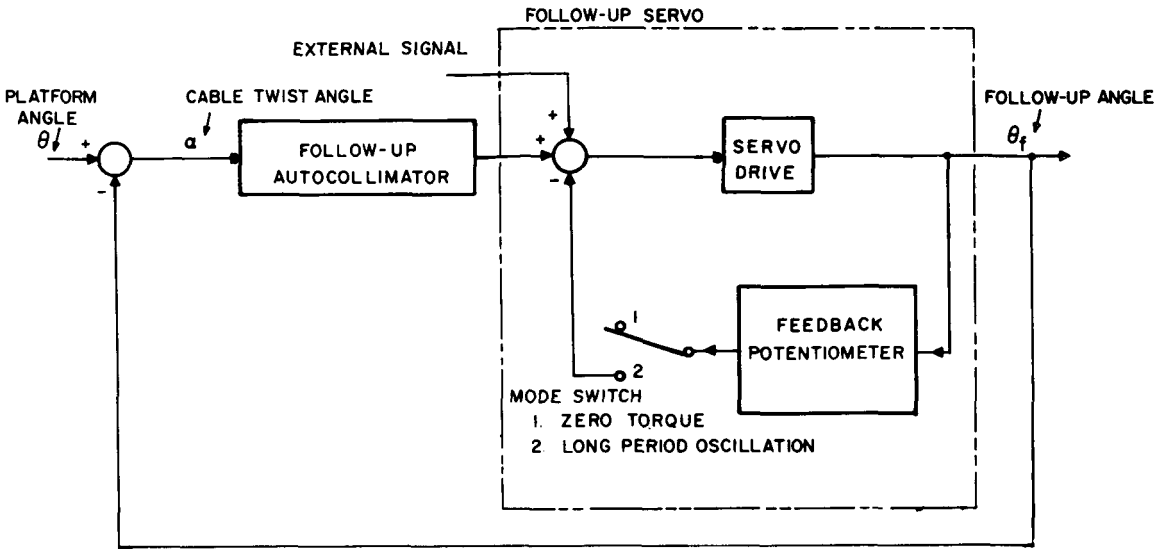

Figure 2. Block Diagram – Zero Torque & Long Period Oscillation Modes

extremely low effective spring constants can be achieved by this artificial softening of the low natural spring constant. This can correspond to very long period oscillations, since the period of oscillation $T = 2\pi\sqrt{\frac{J}{K_e}}$ where J is the platform inertia and K_e is the effective spring constant. Since K_e can be made as low as 0.2% of the natural spring constant K_c, corresponding to a softening factor of 500, the resulting period of oscillation is about 22 times longer than the natural period of oscillation. Periods of oscillation of up to 6 hours and possibly longer can be achieved, provided external disturbance torques (magnetic torques and air currents) can be kept low enough.

Components, such as gravity gradient dampers, that are designed to operate at very low rates and long periods of oscillation can be tested in this long period oscillation mode. For example, the damper can be mounted on the floor with its shaft projecting through the hole in the table. The shaft can be firmly tied to the platform so as to rotate with the platform. When the platform is manually displaced a predetermined angle from equilibrium and then released, the platform will oscillate back and forth extremely slowly and smoothly with the long periods that have been preset into the simulator system. The torques introduced by the damper under test will cause these oscillations to decrease in amplitude, and the rate of decrease is a measure of the damper torques. Or an alternate method which yields faster response in the measurement of torques, is to mount the damper on a sensitive torque measurement device, with the damper shaft tie

to the platform as before. The platform would be initially offset to some predetermined angle as before. As the platform oscillates, the torque measurement device continuously measures the instantaneous torque. This torque signal is also fed to the simulator follow-up drive (at point marked External Signal on Figure 2) such as to counteract the decrease in magnitude of oscillation that would otherwise occur. Thus the long period oscillation can be maintained at some predetermined amplitude while continuous torque measurements of the damper are made.

The second model of the simulator (microthruster table) incorporates the zero torque mode previously described plus a continuous torque mode that permits continuous measurement of torque generated by the microthruster. This latter mode requires an additional electronic autocollimator that is stationary, to measure platform angle θ. This is shown in Figure 3.

Operation in the continuous torque mode is shown in the block diagram of Figure 4. When the component under test produces a torque T_A on the table, the table starts to move through an angle θ. The servo drive receives two oppositely directed signals. One is the signal from the autocollimator measuring cable twist α, which tends to move the follow-up drive in the same direction as table motion. The other signal, from the fixed autocollimator measuring table motion θ, tends to move the follow-up drive opposite to the direction of table motion (in the direction to increase cable twist α). The latter signal is the key to operation in this mode. It is the dominant signal since its gain is much larger (by a factor of about 50) than the signal from the autocollimator measuring cable twist α. Hence, the net result is that the follow-up drive moves rapidly in a direction opposite to table motion θ. This causes a restraining torque on the table, through the cable spring constant, which is opposite in direction to the applied torque from the component under test. Equilibrium is reached when these two torques are equal. The cable restraining torque is proportional to cable twist angle α, which in turn equals platform angle θ minus follow-up angle θ_f. However, because of the very high gain of the fixed autocollimator, the equilibrium follow-up angle θ_f is very much larger than the corresponding platform motion θ. Thus the cable twist α is approximately equal in magnitude to θ_f. Measurement of follow-up angle θ_f then gives an accurate determination of the torque produced by the thruster under test.

A summary of behavior in the continuous torque mode is as follows. Torque generated by the thruster is continuously counterbalanced by a servo produced twist of the cable. This cable twist is essentially all due to servo drive motion θ_f. Measurement of θ_f then enables the determination of thruster produced torque.

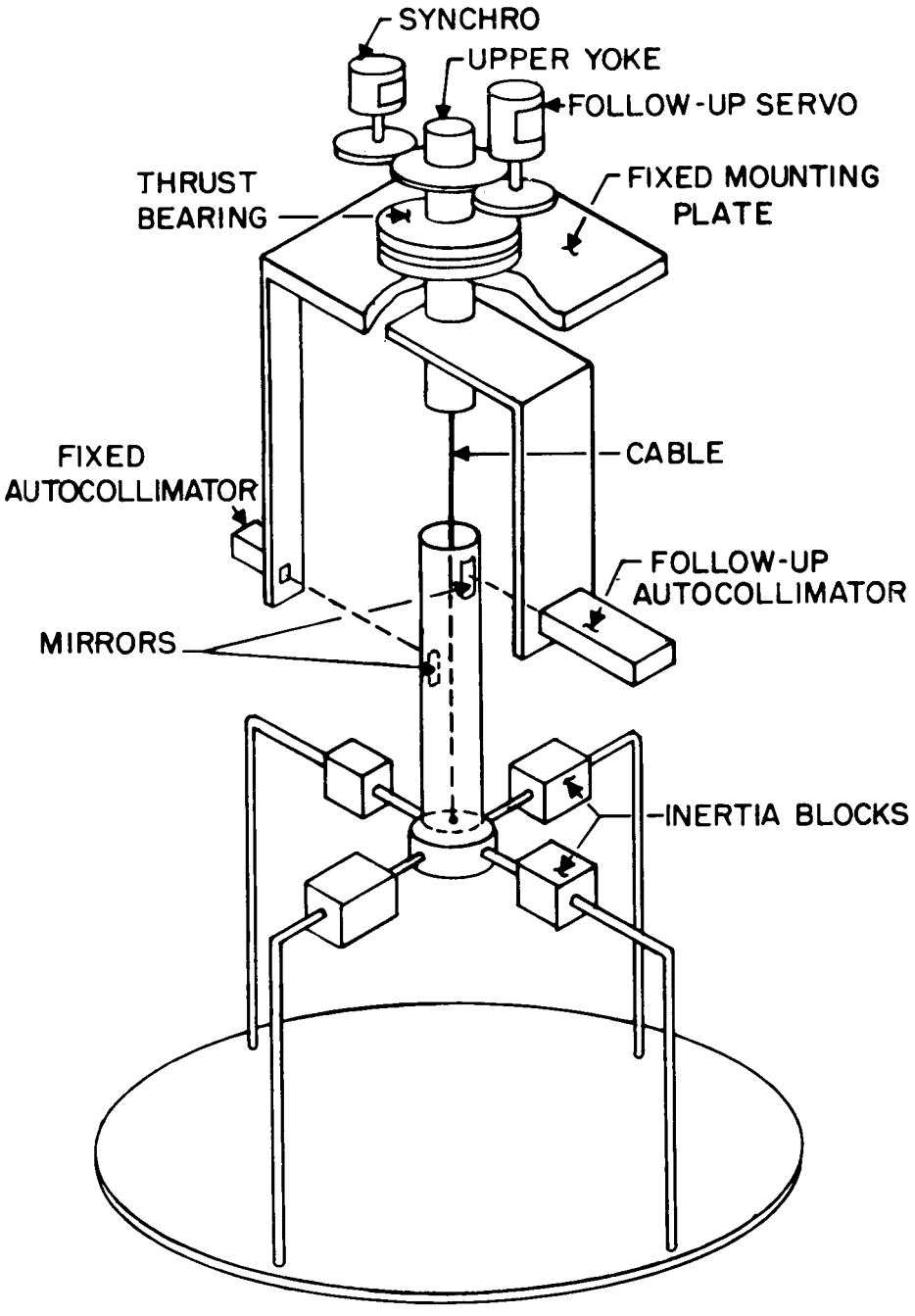

Figure 3. Microthruster Table

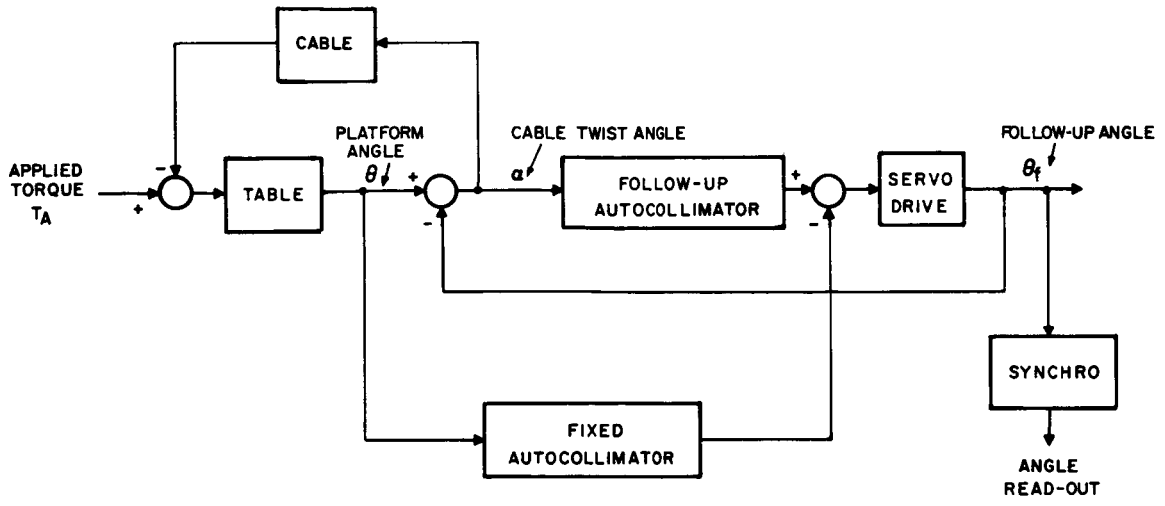

Figure 4. Block Diagram – Continuous Torque Mode

It should be noted that the continuous torque mode is opposite, in a sense, to the long period oscillation mode previously described. In the latter mode, the effective spring constant of the system is greatly reduced, via servo techniques, in order to achieve extremely long periods of oscillation. In the continuous torque mode, the effective spring constant of the system is greatly increased, again via servo techniques, in order to obtain a relatively fast response (0.25 rad/sec) for low level torque measurement. The advantages of using servo techniques to achieve this response, as compared to a purely mechanical torsional spring balance of the proper stiffness, are twofold. First, the servo techniques permit the introduction of artificial damping whereas a purely mechanical system would be extremely oscillatory. Secondly, the measurement of the tiny platform motion θ in an equivalent mechanical system (i.e., having the same natural frequency) would be extremely difficult. In the servo system, it is not necessary to measure this small angle θ. The softness of the cable results in a comparatively large follow-up angle θ_f at equilibrium, which can be measured accurately. Also, small bias errors in the detection of θ by the fixed autocollimator have negligible effect on the follow-up angle θ_f, and hence do not degrade torque measurement accuracy.

III. SINGLE AXIS TABLE DESIGN

A. DESIGN CRITERIA

As discussed previously, the first model built (single-axis table) incorporated the zero torque and long period oscillation modes of operation. The design criteria for this model were the following.

1. Cable load capacity of 500 lbs.

2. Total platform inertia variable up to 100 slug-ft ^{2}.

3. Total height of the facility to be less than 10 feet, so as to be usable in a typical laboratory.

4. A maximum amplitude of oscillation of ±15 deg in the Long Period Oscillation Mode. A maximum period of oscillation up to 6 hours, with the period electronically adjustable over a 2 to 1 range. The amplitude of oscillation to vary less than 1 deg, when there are no external torques on the table.

5. A servo frequency response of 40 rad/sec in the zero torque mode so as to be fast compared to that of the control system under test. (The majority of control systems to be tested have a bandwidth less than 1 cps.) The maximum angular velocity of the servo to be 1 deg/sec. Torque uncertainties due to servo system errors to be less than 10 dyne-cm.

6. The transition from one mode to another should be easily accomplished.

In attempting to meet these criteria, a basic servo system was specified as shown in Figure 5. The cable twist angle α is sensed by an electronic autocollimator and used as the input to the follow-up servo motor. In the zero torque mode, the switch at the feedback potentiometer is open. The integration in $K_2 G_2$ assures zero positional lag error and finite velocity lag error. Hence, in this mode, the wire twist α is reduced to zero except for small errors due to friction, velocity lag, and servo null misalignment. In the long period oscillation mode, the switch is closed, removing the integration in the follow-up servo. Hence the steady state cable twist α becomes proportional to table motion θ, but can be made much less than θ depending on the loop gain.

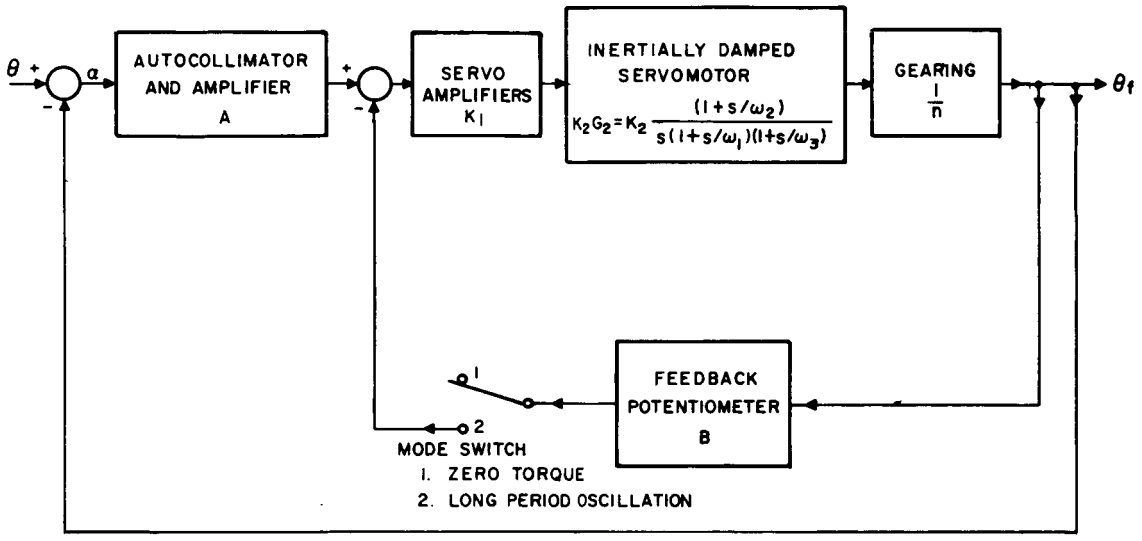

Figure 5. Servo Diagram – Zero Torque & Long Period Oscillation Modes

The following is a typical design procedure that may be used for systems of this type. In practice, the systems were designed using an iterative procedure as is the case for most complicated systems.

B. SERVO SYSTEM DESIGN

In the long period oscillation mode, the feedback potentiometer switch of Figure 5 is closed. Assuming a stable follow-up loop plus $BK_1K_2G_2/n \gg 1$ in the frequency range of interest, we can replace the follow-up loop by $1/B$ in the overall loop analysis. It will be shown later that this assumption is valid.

Hence the overall open loop gain is $KG = A/B$, and the response $\frac{\alpha}{\theta} = \frac{1}{1+KG} = \frac{1}{1+A/B}$.

Let us define a softening factor $S_F = 1 + A/B$. Then $\alpha = \frac{\theta}{S_F}$. Thus for any table angle θ, the cable twist α is less than θ by a factor of S_F. This means that the restraining torque on the table through the cable twist is $T = K_c\,\theta/S_F$, or the effective spring constant $K_e = \frac{T}{\theta} = \frac{K_c}{S_F}$, where K_c is the actual spring constant of the cable. Thus we are theoretically able to obtain an effective spring constant K_e that is less than the cable spring constant K_c by a softening factor S_F.

The design goal of a maximum six hour period of oscillation (with the maximum inertia of 100 slug-ft^2) results in a design goal for K_e of 8.47×10^{-6} lb-ft/rad ($K_e = 3.04 \times 10^{-6} \frac{J}{T^2}$ lb-ft/rad, where J = inertia in slug-ft^2 and T = period

in hours). It is impossible, with any known materials, to design a reasonable length cable to carry 500 lbs which has a spring constant anywhere close to 8.47×10^{-6} lb-ft/rad. One of the best techniques for achieving high load capacity combined with extreme softness, is the use of flat parallel strips of a high tensile strength alloy. This design was used by STL in their single-axis simulator (Reference 1). Reference 2 extends the work of STL to the design of an ultra-soft 52 inch cable capable of carrying 500 lbs. The calculated spring constant for this cable with a 500 lb load is 845×10^{-6} lb-ft/rad. Hence, a value of $S_F = \frac{K_e}{K_c} = 100$ would be required. Larger values of S_F would be acceptable since this would simply mean a smaller inertia to obtain the same period of 6 hours.

The range of softening factor S_F that can be incorporated in the system depends on the linear range and null accuracy of an available electronic autocollimator. The maximum value of S_F is a function of the autocollimator null error e_n (resolution plus drift) since this error is multiplied by S_F in forming the equivalent table error. It was considered desirable to limit this contribution to table error to about 1/3 degree or less, which meant $S_F e_n < 1200$ arc-sec. The minimum value of S_F is a function of the linear range of the autocollimator, since a ±15 deg range of table oscillation results in a range of cable twist α given by $\alpha = \frac{15\,\text{deg}}{S_F}$. If possible, the range of S_F should be 4 to 1 in order to allow a 2 to 1 range in frequency of oscillation, without any mechanical changes.

An electronic autocollimator was found (H-H Controls Co. Refractosyn) that meets these constraints. In addition, the autocollimator has a desirable high sensitivity to angular rotation about the primary axis, and a relatively low sensitivity to rotation about the remaining two axes as well as to linear displacement. This autocollimator has a measured total null error of 2½ arc-sec or less and a linear range of about 7½ arc-min. This permits a range of S_F from 120 to 480, which meets the desired 2 to 1 range of variation of table period electronically. Of course, a much larger range in table period is still inherent in the simulator design through the use of lower table inertia and/or stiffer cable.

Having selected $S_F = 1 + A/B \approx A/B$ to be adjustable over the range from 120 to 480, there remains the question of selecting the values of A, B, and the servo characteristic $K_2 G_2$. It was deemed desirable to restrict all gain adjustments, in both the long period oscillation and zero torque modes, to the autocollimator gain box A. Also the servo loop consisting of A and $K_1 K_2 G_2/n$ had to meet the zero torque mode requirement of 40 rad/sec bandwidth.

A first step in the servo system design was the selection of a 400 cps inertially-damped servo motor with a characteristic

$$K_2 G_2 = \frac{7}{s} \times \frac{(1 + s/7.54)}{(1 + s/1.88)(1 + s/160)} \frac{\text{rad/sec}}{\text{volt}} \quad \text{(Kearfott R1310-2B).}$$

The choice was based primarily on obtaining a motor with corner frequencies that would be compatible with a zero torque mode bandwith of 40 rad/sec. Of course, suitable gearing is required to minimize the load inertia reflected back to the motor, in order to maintain the high frequency corner. A big advantage in using an inertially damped servomotor is that it eliminates the need for any additional stability networks.

Secondly, to eliminate the need for demodulating and remodulating the autocollimator output, the autocollimator was obtained with lamp filaments capable of responding to a 400 cycle, half-wave rectified sine wave. In addition to preserving the insensitivity of the autocollimator to ambient light, this enabled the autocollimator to deliver a 400 cps error signal which after appropriate amplification, and phase correction, could be fed directly to the follow-up servo.

The starting voltage for the motor and gear train was measured to be about 4 volts. Calling the equivalent striction error e_s (referred to the cable), we have the following relation for equivalent table error in the long period oscillation mode.

$$\theta_s = S_F e_s = \frac{A}{B} e_s.$$

But e_s is simply $\frac{4 \text{ volts}}{AK_1}$. Hence,

$$\theta_s = \frac{A}{B} \times \frac{4 \text{ volts}}{AK_1} = \frac{4 \text{ volts}}{BK_1}$$

In order to limit this table error component to about 1/3 degree (5.9×10^{-3} rad), BK_1 should be

$$BK_1 = \frac{4 \text{ volt}}{5.9 \times 10^{-3} \text{ rad}} = 0.68 \times 10^3 \frac{\text{volts}}{\text{rad}}$$

This was accomplished by selecting the servo amplifier gain K_1 at 34 and feedback potentiometer gain B at 20 volts/rad.

The required range for A is now determined by the desired range for S_F (120 to 480). Since $S_F = \frac{A}{B} = \frac{A}{20 \text{ volts/rad}}$, we have

$$A \text{ min} = 20 \frac{\text{volts}}{\text{rad}} \times 120 = 2400 \frac{\text{volts}}{\text{rad}} .$$

$$A \text{ max} = 20 \frac{\text{volts}}{\text{rad}} \times 480 = 9600 \frac{\text{volts}}{\text{rad}} .$$

In the zero torque mode an overall gain $K = 160 \text{ sec}^{-1}$ ($K = AK_1K_2/n$) is required in order to achieve a 40 rad/sec bandwidth. With A set at its maximum value, to minimize stiction, we have as the required gearing ratio

$$n = \frac{AK_1K_2}{K} = \frac{9600 \times 34 \times 7}{160} = 14,300$$

A gearing ratio of 14,000 was selected for the servo drive.

We can now check the stability of the various loops in the long period oscillation mode. The open loop gain of the minor loop (follow-up servo) is

$$K_3G_2 = \frac{BK_1K_2}{n} G_2.$$

Using the previously selected values for B, K_1 and n, together with the servomotor characteristic K_2G_2, we obtain

$$K_3G_2 = \frac{0.34 \text{ sec}^{-1}}{s} \frac{(1 + s/7.54)}{(1 + s/1.88)(1 + s/160)}$$

A Bode plot of minor loop gain K_3G_2 is shown in Figure 6. This indicates good stability (phase margin = 82 deg) and a satisfactory bandwidth (zero db frequency $\approx$ 0.34 rad/sec). The bandwidth is sufficiently high since the highest frequency of oscillation in the long period oscillation mode is expected to be less than 1 cycle/0.5 hrs $\approx 3.5 \times 10^{-3}$ rad/sec. The closed loop response is also shown in Figure 6 in terms of B $\times$ closed loop response.

The major open loop gain is given by A $\times$ closed minor loop or $\frac{A}{B} \times$ (B $\times$ closed minor loop), where $\frac{A}{B} = S_F$ (softening factor). Hence, the major open loop characteristics can be plotted by multiplying (B $\times$ closed minor loop) by the extremes of S_F, namely 120 and 480. This is shown in Figure 7. Good stability

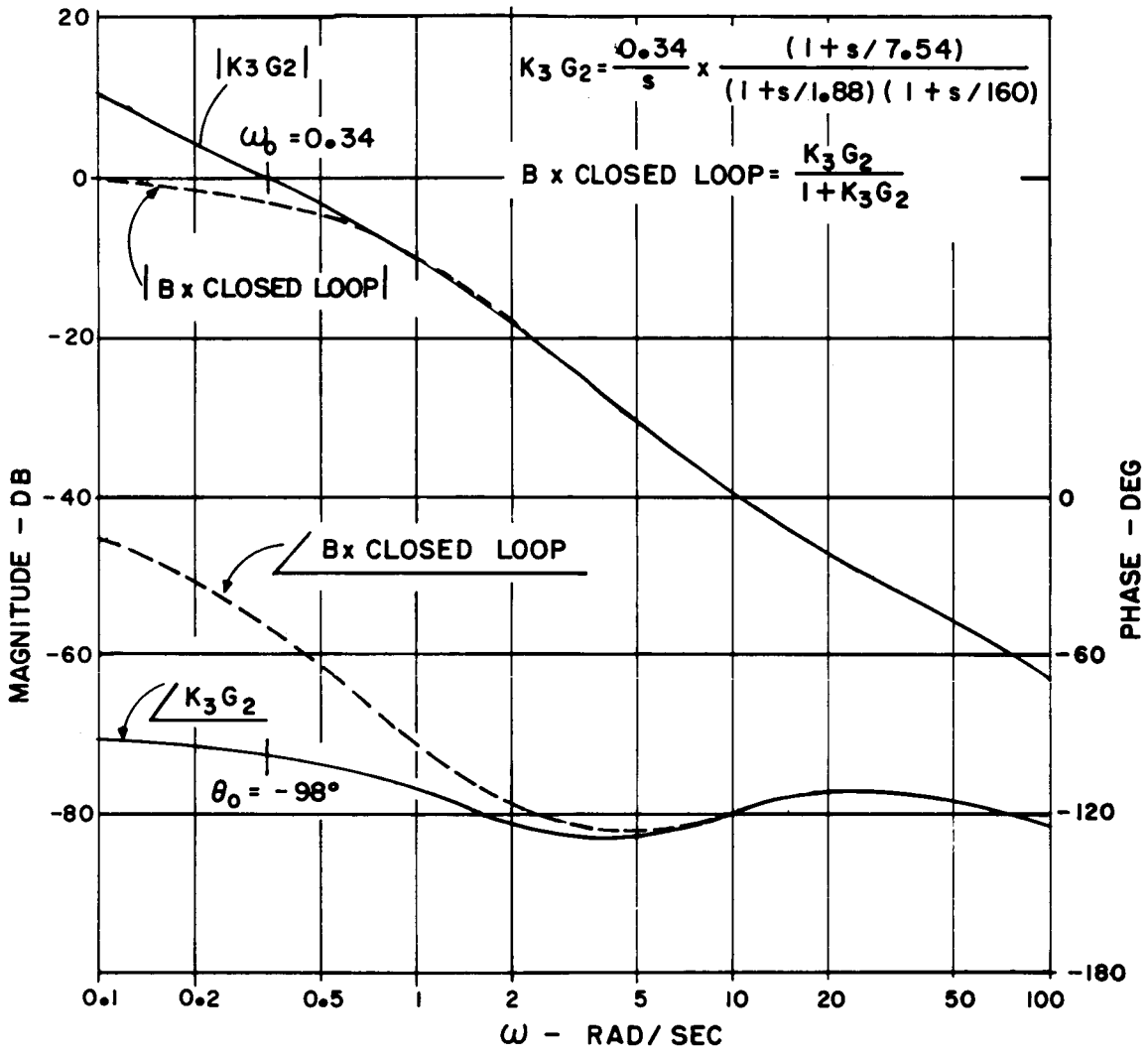

Figure 6. Follow-up Servo Bode Diagram

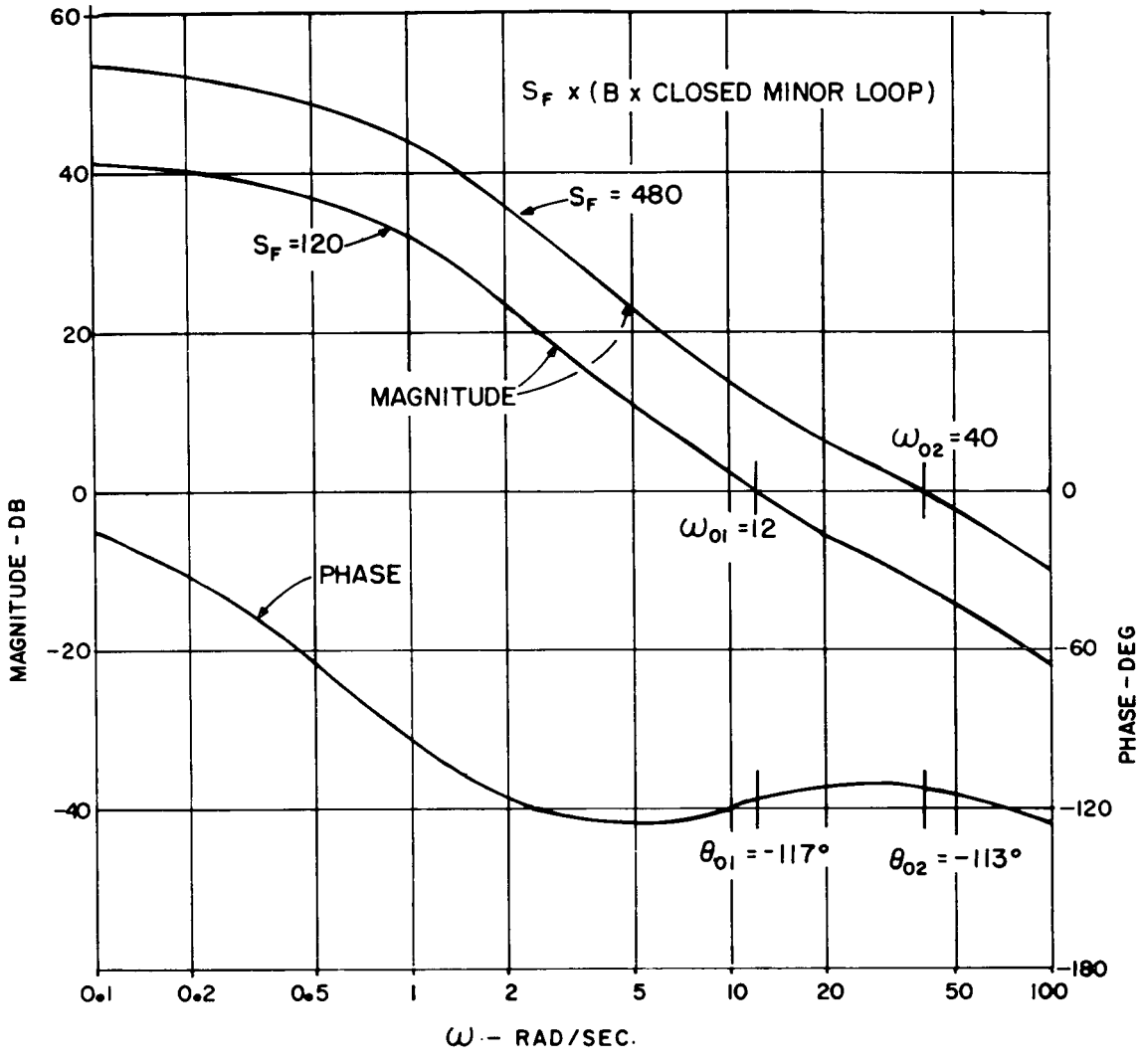

Figure 7. Bode Diagram – Single Axis Table

is obtained at both extremes as well as for the range in-between (minimum phase margin $\approx$ 63 deg). Also the minimum bandwidth of 12 rad/sec is more than ample for the long period oscillation mode.

The following table summarizes the basic servo characteristics in the long period oscillation mode.

Characteristic	S_F = 120	S_F = 480
Pot Feedback gain B	20 volts/rad	20 volts/rad
Minor loop gain K_3	0.34 sec^{-1}	0.34 sec^{-1}
Minor loop phase margin	82 deg	82 deg
Variable gain A	2400	9600
Softening factor $S_F = \frac{A}{B}$	120	480
Major loop phase margin	63 deg	67 deg
Major loop bandwidth	12 rad/sec	40 rad/sec
Autocollimator null error	2.5 arc-sec	2.5 arc-sec
Servo stiction error	10 arc-sec	2.5 arc-sec
Total servo error	12.5 arc-sec	5 arc-sec
Equivalent torque error (for 500 lb load)	0.69 dyne-cm	0.28 dyne-cm
Equivalent table error	0.42 deg	0.67 deg

(S_F = Softening Factor)

These characteristics meet the applicable design criteria for the long period oscillation mode. With no external torques on the table, the variation of table amplitude should be no worse than ±0.7 degrees. Misalignment errors between the autocollimator null and the cable null were not included in the above since these produce a constant bias offset of the center of oscillation. Of course such

misalignment errors must be kept within reasonable limits to stay within the linear operating range of the system.

The adjustment of S_F between 120 and 480 permits a 2 to 1 variation in table period electronically. For a given table inertia J and cable spring constant K_c, the frequency of table oscillation in rad/sec would be simply $\omega = \sqrt{\frac{K_e}{J}}$ where $K_e = \frac{K_c}{S_F}$.

In the zero torque mode, the system is operated with the potentiometer feedback loop open (See Figure 5). The servo gain in this mode is simply KG_2 where $K = AK_1K_2/n$. As discussed earlier, the gain K was selected to be 160 sec^{-1} in order to obtain a bandwidth of 40 rad/sec in this mode. The value of A corresponding to this gain is 9600 volts/rad. A check of the stiction error in the zero torque mode shows that

$$e_s = \frac{4 \text{ volts}}{AK_1} = 2.5 \text{ arc-sec.}$$

This represents an insignificant torque error.

Another error in the zero torque mode results from the velocity following error at maximum speed of 1 deg/sec. Since the velocity constant is K = 160 sec^{-1}, the following error at 1 deg/sec is simply

$$e_v = \frac{1 \text{ deg/sec}}{160/\text{sec}} = \frac{1}{160} \text{ deg} = 22.5 \text{ arc-sec.}$$

Combining this error with the stiction error of 2.5 arc-sec and the autocollimotor null error of 2.5 arc-sec results in a maximum random servo error of 27.5 arc-sec. With the estimated spring constant of 845×10^{-6} ft-lb/rad $\approx 0.055 \frac{\text{dyne-cm}}{\text{arc-sec}}$, the total error is equivalent to a maximum servo torque error of only 1.5 dyne-cm. (This, of course, does not include external torques due to thermal air currents or other disturbances.)

In addition to the random error of 1.5 dyne-cm, there is a constant bias error due to mechanical misalignment between the autocollimator null and the servo null. The autocollimator position can be adjusted mechanically via two micrometer heads that permit all backlash to be removed. However, it is not practical to set the micrometers closer than 0.001 inch which corresponds to an angle of about 100 arc-sec. With the above spring constant of 0.055 dyne-cm this corresponds to a constant torque bias of 5.5 dyne-cm. For greatest accuracy

in determining torque produced by a component under test, this bias torque can be measured and subtracted from the measured torque. However, even if this is not done, the total servo system error would only amount to (5.5 + 1.5) dyne-cm or 7 dyne-cm. Thus the servo system design more than satisfies the requirements for operation in the zero torque mode.

It should be noted that the basic system design allows for easy changeovers from one mode of operation to another. All that is required to change from the long period oscillation mode to the zero torque mode is to open up the potentiometer feedback loop and to readjust the variable gain A to the predetermined value of 9600 volts/rad.

C. ELECTRO-MECHANICAL DESIGN

As seen in Figure 1 the table is suspended on a cable from an upper yoke. The cable is made of a number of ribbons of a very high strength nickel-cobalt alloy. It is designed to have a very low torsional spring constant (see Reference 2). The upper yoke is supported by a low torque thrust bearing and has unlimited freedom of rotation.

The follow-up autocollimator is mounted on a plate attached to the upper yoke and therefore rotates with it. Fine adjustment of the autocollimator about the vertical axis is achieved by two micrometer heads which position it with respect to the upper yoke. The power and signals for the autocollimator and its associated electronics are routed through the upper yoke and attached slip rings. The sighting mirror for the autocollimator is attached to a tube surrounding, but not touching the cable. This tube is rigidly mounted to the table (Figure 1). Thus the sensor measures the twist angle α between the top of the cable and the bottom.

The drive for the upper yoke consists of a motor-gearbox package which drives the yoke by means of a friction drive. A friction drive was used to insure a smooth motion free of backlash. The 1000:1 gear train is of precision three quality. The equivalent backlash through the entire drive (14,000:1) is less than 5 seconds of arc, referred to the output axis.

A synchro is also connected to the upper yoke by means of a 1:10 friction drive. The synchro position, accurate to 0.1°, is displayed on the control console. Due to the 1:10 ratio between the yoke and synchro, the control console readout gives the upper yoke position to 0.01°.

Three tables are available for use with this system. One is a light duty (150 lb capacity), 3½ ft diameter table which is completely non-magnetic and is

used only in the zero torque mode. The other two tables are heavy-duty (500 lb load capacity), having diameters of 4 ft and 6 ft respectively, and were designed for use in either the zero torque or long period modes. These two tables can be adjusted in inertia via brass weights that are attached at the table perimeter. The total range of inertia for the two heavy duty tables is from 8.7 to 100 slug-ft ^{2}.

Figure 8 is a schematic of the system. All the amplifiers are modular types. Due to a thermal lag in the sensor lamp the sensor amplifier output carrier is out of phase with the reference carrier. The carrier phase adjust circuit is included to account for this. All the mode control switches are on the control panel. The components from the follow-up sensor through the follow-up input switch form the gain A of Figure 5. The servo preamplifier, amplifier, and transformer of Figure 8 are equivalent to gain K_1 in Figure 5. The mode switch in both figures is just ahead of the summing function. Finally, the feedback pot, clutch, and associated gearing form gain B of Figure 5.

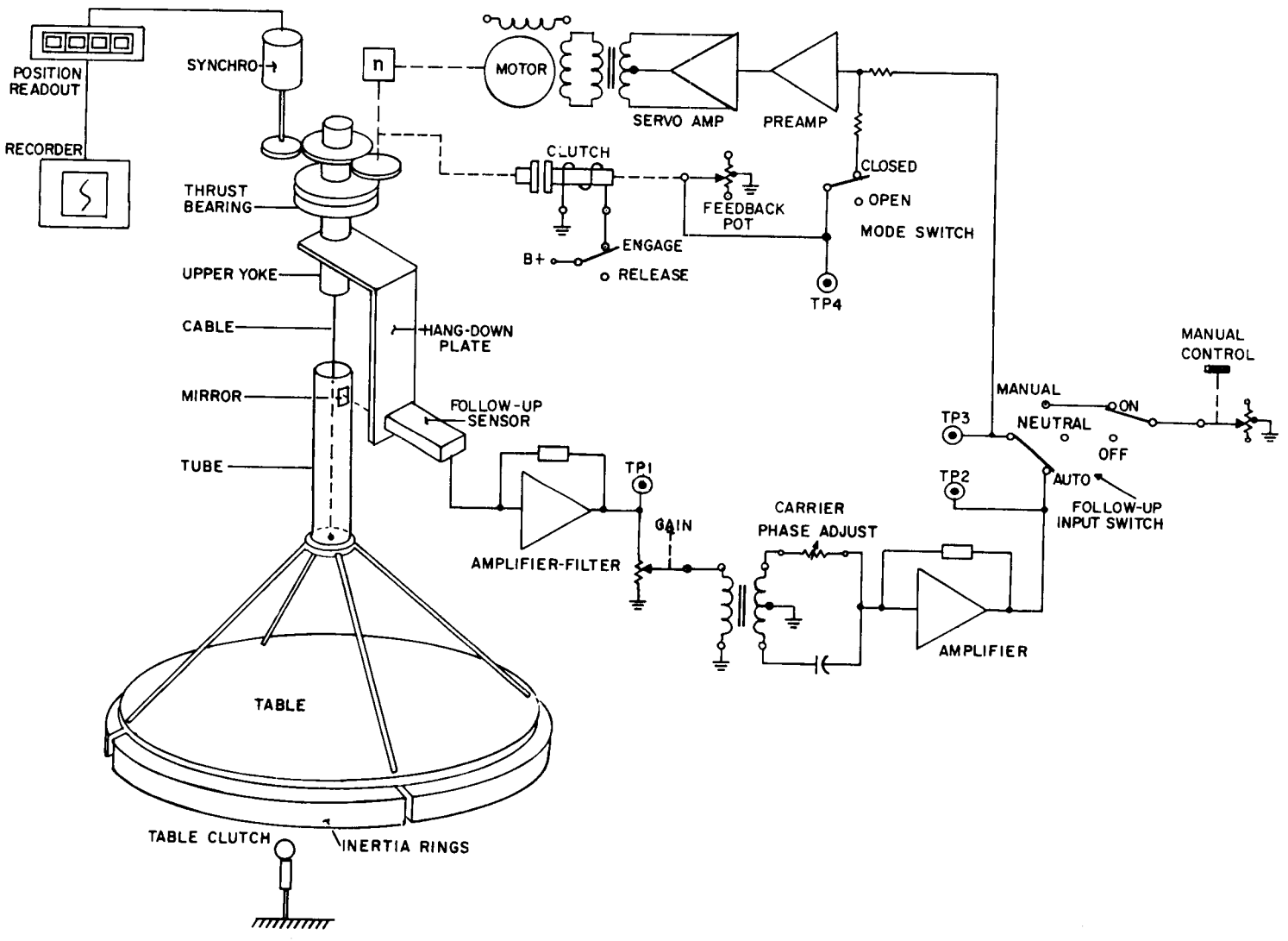

Figure 8. Schematic Diagram – Single Axis Table

IV. MICROTHRUSTER TABLE DESIGN

A. DESIGN CRITERIA

One purpose of the microthruster table is to measure accurately the thrust of microthruster engines in the range of 10 to 200 micropounds. A second goal is to measure the closed loop performance of microthruster control systems in a single-axis mode of operation. To meet these goals, the basic single-axis simulator concept was adopted, to provide a zero torque environment for the platform on which the engine or engine control system is to be mounted. In addition, the concept was extended to include a continuous torque mode, to permit "instantaneous" measurement of torque, in a torque balance type of operation. In addition to incorporating these two modes of operation, the microthruster table was required to meet the following design criteria.

1. The table should be capable of operating in a vacuum chamber at vacuums as low as 10^{-6} mm of Hg.

2. The platform should be capable of supporting 100 lbs of equipment (engine, engine auxiliary equipment, batteries, telemetry, command receiver, etc.).

3. The entire system should fit within a 4 ft diameter cylinder (approximate diameter of available vacuum chamber).

4. The design should permit the substitution of larger platforms with load capacity up to 400 lbs. (Of course, a larger vacuum chamber would be required in which to operate the system.)

5. The system to have a torque measurement range of 140 to 1400 dyne-cm with a measurement accuracy of 5% at any torque within this range. (10 micropounds at 1' radius is about 140 dyne-cm; 200 micropounds at 0.5' radius is about 1400 dyne-cm. Thus a 2' diameter platform would permit thrust measurements of engines from 10 to 200 micropounds, at reasonable radii.)

6. The bandwidth in the zero torque mode to be at least 40 rad/sec, in order to be fast compared to the bandwidth of control systems under test.

7. The bandwidth in the continuous torque mode to be at least 0.5 rad/sec, for the 100 lb load configuration.

8. The system should be easily changed from the zero torque mode of operation to the continuous torque mode, and vice-versa.

B. SERVO DESIGN

The basic servo system shown in Figure 9 was selected as compatible with the design goals previously listed.

In the zero torque mode the system is essentially identical to the zero torque mode of the single-axis table which was previously described. It should be noted that this mode is essentially independent of the size of platform used, since this mode merely nulls the cable twist to provide a zero torque environment for the platform. The only effect of platform size is the effect of platform weight on cable spring constant which in turn determines the amount of torque bias caused by servo system errors. Also the length of cable has a similar effect on the resultant torque bias errors. In the case of the microthruster table, the size limitation limited the cable length to only 10" compared to the 52" cable on the larger simulator. While this effect in itself would increase the spring constant, the much smaller weight of the microthruster table permitted a thinner cable in the zero torque mode so that the net result was a smaller cable spring constant (0.036 dyne-cm/arc sec). Thus the total servo system error of 28 arc sec in the zero torque mode results in a torque bias error of about 1 dyne-cm. This is less than 1% of the minimum value of torque to be measured (140 dyne-cm), which is compatible with the required overall torque measurement accuracy of 5%.

In the continuous torque mode of operation, (see Figure 9) the servo equation relating θ_f to θ can be developed as follows:

Let $K = \frac{AK_1K_2}{n}$.

Then KG_2 = open loop gain characteristic of zero torque mode (bandwidth $\approx$ 40 rad/sec).

$$\theta_f = \frac{KG_2}{1 + KG_2}\,\theta - \frac{KG_2}{1 + KG_2}\,\frac{B}{A}\,(1 + Ts)\,\theta$$

Since the specified system bandwidth is 0.5 rad/sec in the continuous torque mode, and since $KG_2/(1+KG_2) = 1$ for frequencies up to 40 rad/sec, we can simplify the above equation to the following.

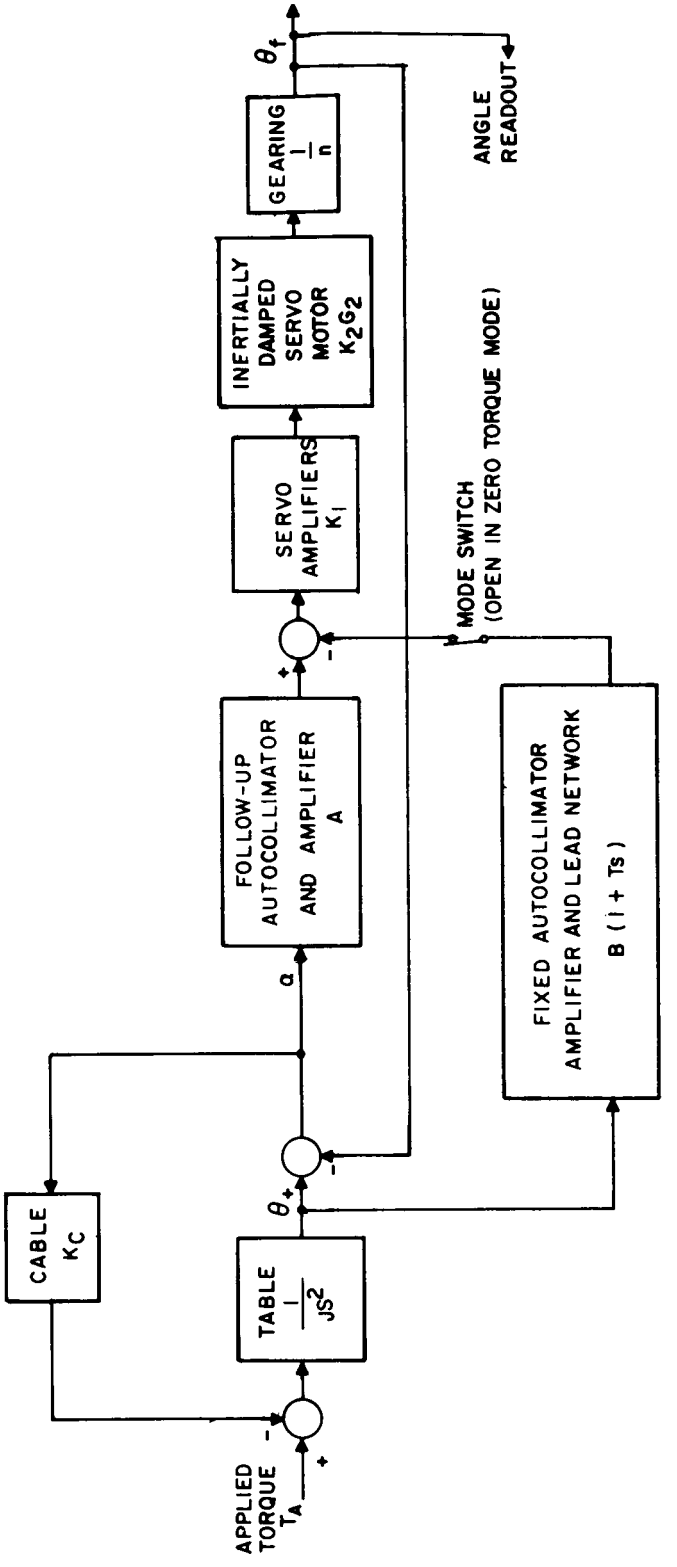

Figure 9. Servo Diagram – Continuous Torque Mode

$$\theta_f = \theta - \frac{B}{A}(1 + Ts)\ \theta$$

The factor B/A can be made very large compared to unity. Hence, we can obtain

$$\theta_f \approx - \theta \frac{B}{A}(1 + Ts)$$

With this simplification, the servo block diagram reduces to that shown in Figure 10a.

Referring to this diagram, we can see that

$$\alpha = \left[1 + \frac{B}{A}(1 + Ts)\right]\theta$$

But B/A >> 1. Hence

$$\alpha \approx \frac{B}{A}(1 + Ts)\ \theta$$

and the servo diagram reduces to that shown in Figure 10b.

Thus the final open loop gain characteristic in the continuous torque mode is simply

$$GH = \frac{K_c}{Js^2}\ \frac{B}{A}(1 + Ts)$$

The characteristic equation is then

$$1 + \frac{K_c}{Js^2}\ \frac{B}{A}(1 + Ts) = 0$$

or,

$$s^2 + \frac{B}{A}\frac{K_c\, Ts}{J} + \frac{B}{A}\frac{K_c}{J} = 0$$

This is of the standard quadratic form $s^2 + 2\zeta\omega_n s + \omega_n{}^2 = 0$

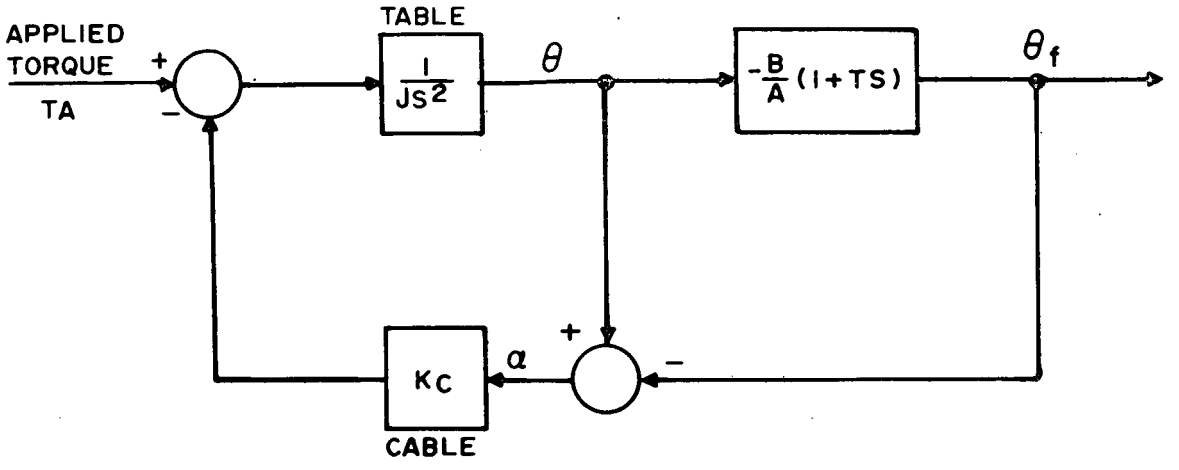

(a)

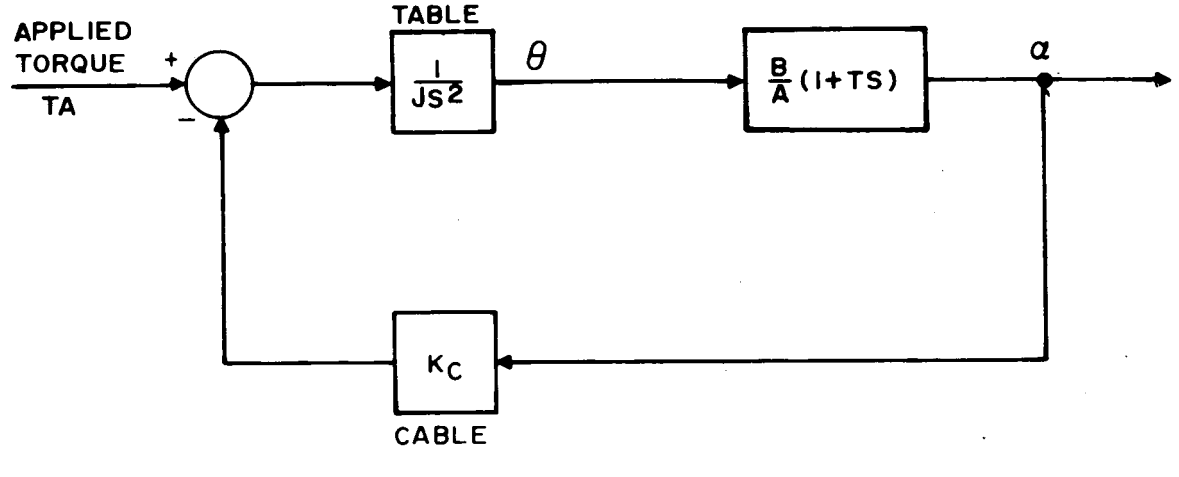

(b)

Figure 10. Continuous Torque Mode – Simplified Servo Diagrams

Therefore

$$\omega_n^2 = \frac{B}{A}\frac{K_c}{J} = \frac{B}{A}\omega_{no}^2$$

$$2\zeta\omega_n = \frac{B}{A}\frac{K_c T}{J} = \omega_n^2 T$$

$$\zeta = \frac{\omega_n T}{2}$$

where $\omega_{no} = \sqrt{K_c/J}$ is the undamped natural frequency of the cable-platform combination.

Thus, it is seen that we can artificially obtain critical damping for the system, and operate at a system natural frequency ω_n that is much higher than the natural frequency associated with the soft cable and platform inertia. As long as ω_n is much smaller than the zero torque bandwidth of 40 rad/sec, the preceding analysis is valid.

The desired torque measurement range is from 140 to 1400 dyne-cm. With the very soft cable of the zero torque mode ($K_c \approx 0.036$ dyne-cm/arc/sec), this would result in a maximum steady-state cable twist of α equal to 650 arc-min. This is well outside the linear range of the electronic autocollimator (7 arc-min). The preceding analysis assumes linear operation of the autocollimators. Also, the extremely soft cable would result in a very low natural frequency ω_n, even taking into account the multiplication factor of $\sqrt{B/A}$. A satisfactory compromise was achieved by utilizing a somewhat stiffer cable ($K_c \approx 0.36$ dyne-cm/arc-sec). This results in a maximum cable twist of α equal to 65 arc-min. However, this range was extended optically beyond 70 arc-min, via an additional servo drive, to be described later.

The maximum load capacity of 100 lbs results in a maximum inertia of about 4 slug-ft^2. This, together with the cable spring constant of 0.36 dyne-cm/arc-sec (5.5×10^{-3} lb-ft/rad), results in a mechanical natural frequency of $\omega_{no} = 0.037$ rad/sec. Since the system natural frequency is $\omega_n = \sqrt{B/A}\,\omega_{no}$, it is desirable to utilize as large a factor B/A as possible, consistent with various constraints. These constraints are to limit the resolution errors in cable twist α due to a finite resolution of the fixed autocollimator, and to insure that the system natural frequency is still small compared to the zero torque bandwidth of 40 rad/sec. A value of B/A of 50 was selected as consistent with these constraints. It results in a multiplication factor of 7 for the system natural frequency, or $\omega_{n_{min}} \approx 0.25$ rad/sec.

The pure lead term $(1 + TS)$ cannot be achieved practically but can be approximated effectively by a lead term of the form $\frac{(1 + TS)}{(1 + \gamma TS)}$ where $\gamma << 1$. Even though the value of T for critical damping varies with system natural frequency, it was felt that a single value of T could provide good stability over the 8 to 1 range of inertia. A value of $T = 4.35$ sec and $\gamma = 0.046$ was selected. The resultant Bode diagram for the torque loop (Figure 11) shows that good stability can be achieved over the full range of inertias with a minimum bandwidth of 0.3 rad/sec. The minimum phase margin over the entire range is about 44 degrees. (In the case of a major change in inertia, such as going to a larger platform with larger load capacity, the value of T would have to be adjusted to suit the new range of inertias.)

As discussed previously, the torque produced by the engine under test is counterbalanced at servo equilibrium, by the torsion in the cable due to cable twist. Thus torque $= K_c \alpha = K_c (\theta - \theta_f)$ (referring to Figure 9). At equilibrium, $\theta_f = -\frac{B}{A} \theta \approx -50\ \theta$, or $\theta_f >> \theta$. Hence, as an approximation, torque $\approx -K_c \theta_f$, or if we wish to be more exact, torque $= -K_c \theta_f (1 + A/B) = -1.02\, K_c \theta_f$. In either case, measurement of follow-up angle θ_f, at servo equilibrium results in a measurement of applied torque. The angle is measured by a synchro with a resolution (via gearing) equivalent to 0.001 deg (3.6 arc-sec) of follow-up angle.

An error analysis of the continuous torque mode indicates that the measurement of θ_f will be in error by no more than 14 arc-sec, which is equivalent to a torque uncertainty of 5 dyne-cm. This amounts to 3.6% of the minimum torque to be measured. In addition, there is an estimated 2% inaccuracy in determining the cable spring constant K_c. Hence, the total torque measurement accuracy is estimated to be 5.6% at 140 dyne-cm. At 1400 dyne-cm, the accuracy is about 2.4%.

C. ELECTRO-MECHANICAL DESIGN

The microthruster table is basically a small vacuum chamber version of the single axis table (see Figure 3). For this reason, many of the mechanical and electrical features of the system are similar or even identical. The basic differences are discussed in the following paragraphs.

All of the bearings and each mesh in the gear train were lubricated with silicon lubricant for vacuum operation. The position readout synchro, accurate to 0.1 degrees, was incorporated in this gear train with a 1:100 gear ratio to the upper yoke. Thus, the upper yoke position (θ_F) can be measured to 0.001 deg or 3.6 arc-seconds.

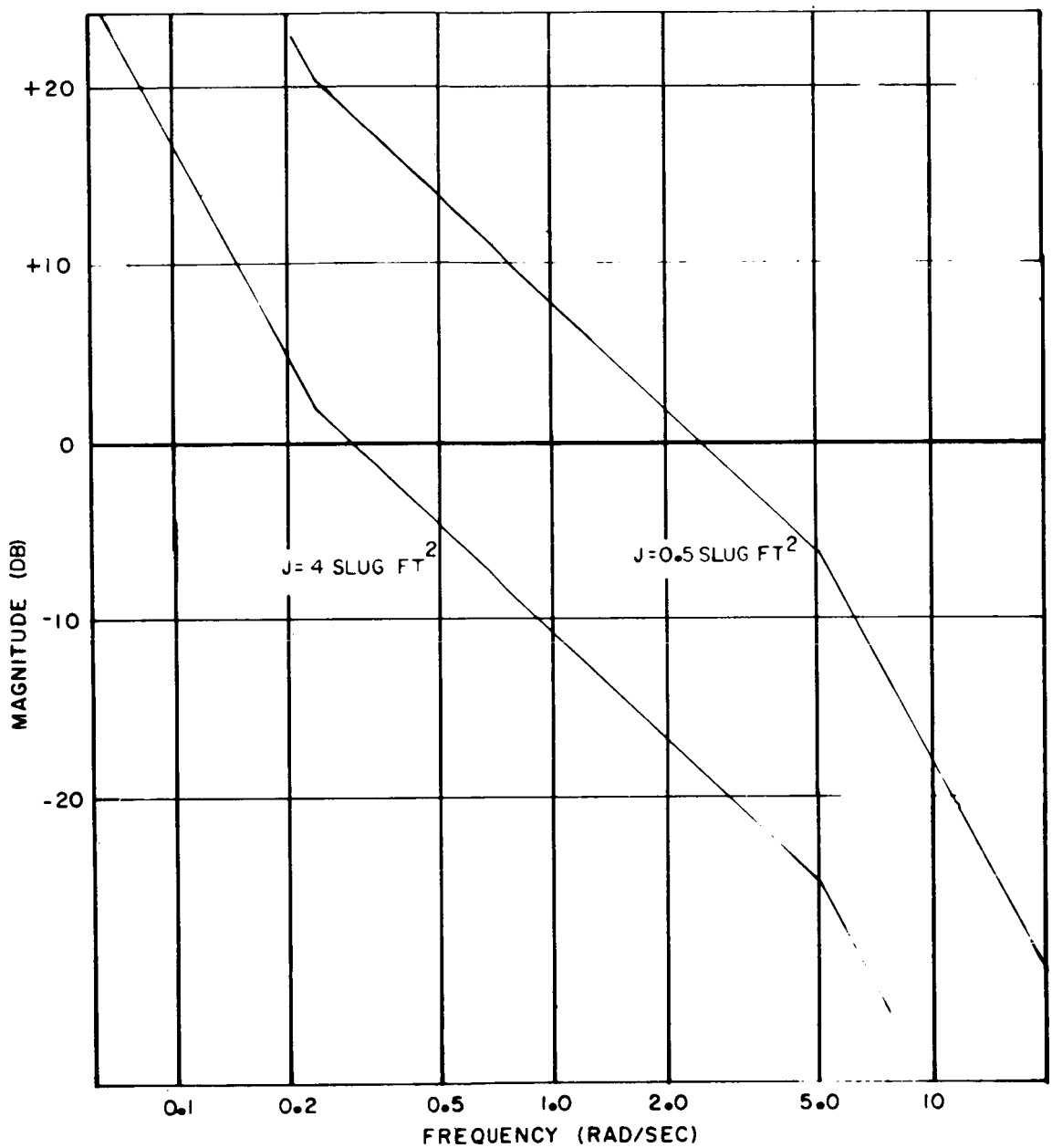

Figure 11. Bode Diagram – Continuous Torque Mode

The design for the continuous torque mode of operation required an additional fixed autocollimator to measure table motion θ. This is shown in Figure 3. This fixed sensor is basically the same as the follow-up sensor. The error signal is boosted immediately following the sensor before being routed to the control console.

In the continuous torque mode, the cable twist α counterbalances the applied torque T_A. This angle α is measured by the follow-up autocollimator. However, for the maximum torques to be measured, this angle can be as high as one degree, which is well beyond the linear range of the sensor. To circumvent this difficulty, the subtraction shown prior to the servo amplifier in Figure 9 was done optically within the follow-up sensor. The follow-up sensor output was therefore operated near its null condition.

The optical subtraction was implemented as follows (see Figures 9 and 12). The follow-up sensor output signal directly feeds the preamplifier A which directly feeds servo amplifier K_1. This sensor output signal is controlled by two inputs. One is the twist α of the cable which changes the angular position of the collimator mirror by an equal amount. The second input is the angle β of a glass slab within the follow-up sensor which changes the angle of the collimating beam proportional to β. This linear relationship holds up to about ±25 deg motion of the slab. The gain of this input relative to mirror motion α is a function of the slab width used. The selected slab results in a gain of 0.1, which means

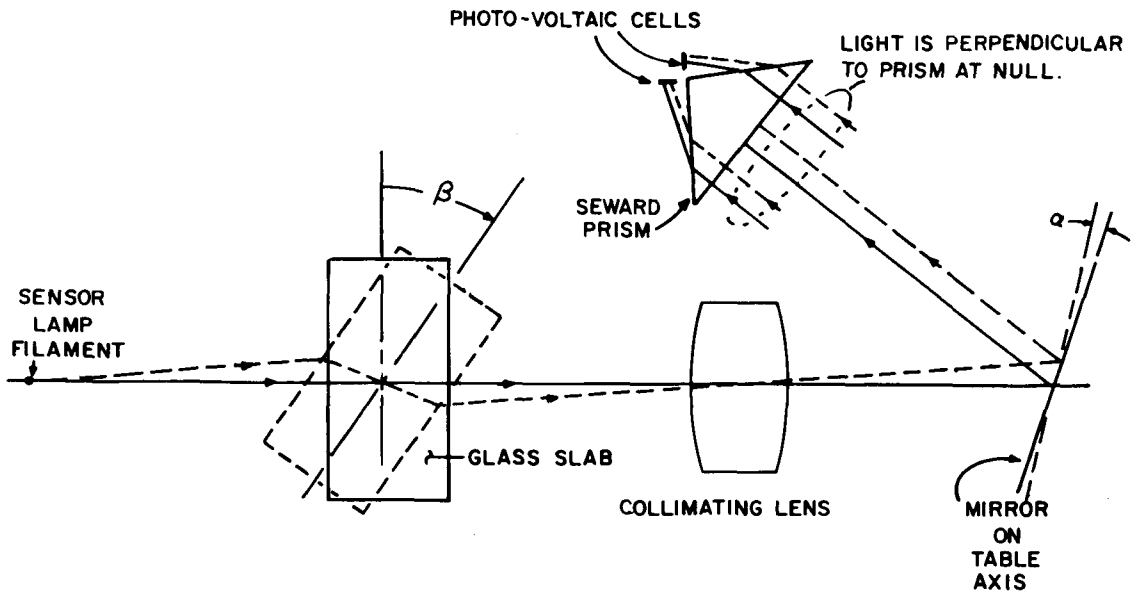

Figure 12. Schematic of Autocollimator Optics

that a slab rotation β = 10 deg is equivalent to a wire twist (or mirror motion) α = 1 deg. The slab is driven by a small servo controlled from the fixed autocollimator output. Thus, the follow-up sensor output is made to represent the difference between the two inputs.

The follow-up sensor output signal will be driven to null due to the integration in the follow-up servomotor (K_2G_2). Thus, the linear range of the follow-up sensor has been effectively extended to ±2.5 deg, corresponding to the linear range of ±25 degrees for slab angle β.

It should be noted that the summation in Figure 9 between blocks A and K_1 has actually been carried out within the follow-up sensor prior to block A. To keep the system equivalent to the servo diagram of Figure 9, the fixed autocollimator block was mechanized as $\frac{B}{A}(1 + Ts)$. That this is an equivalent system is easily shown. From Figure 9 the input to K_1 is $A\alpha - B(1 + Ts)\theta$. The input to K_1 in the actual system is $A\left[\alpha - \frac{B}{A}(1 + Ts)\theta\right]$. These two expressions are obviously identical.

In the schematic diagram of Figure 13, the components from the follow-up sensor through the follow-up input switch form the gain A. The servo preamplifier, amplifier, and transformer form the gain K_1. The components from the fixed sensor through the slab drive servo, including the optical gain (0.1) within the follow-up sensor, constitute the transfer function $\frac{B}{A}(1 + Ts)$.

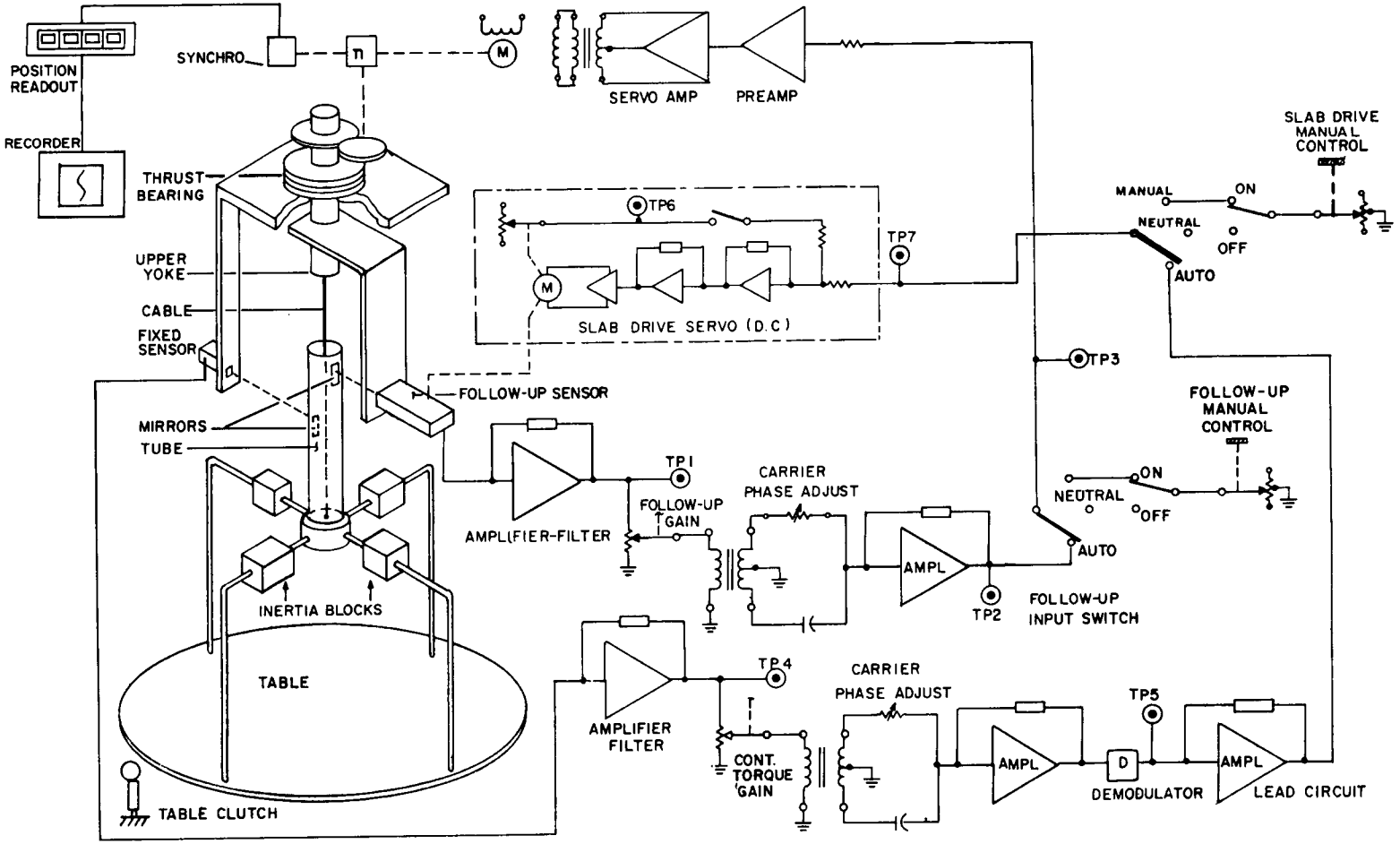

Figure 13. Schematic Diagram – Microthruster Table

V. TELEMETRY SYSTEM

The telemetry transmission system for each table is shown in Figure 14. It is a standard PDM/FM/FM system employing FM channels at conventional

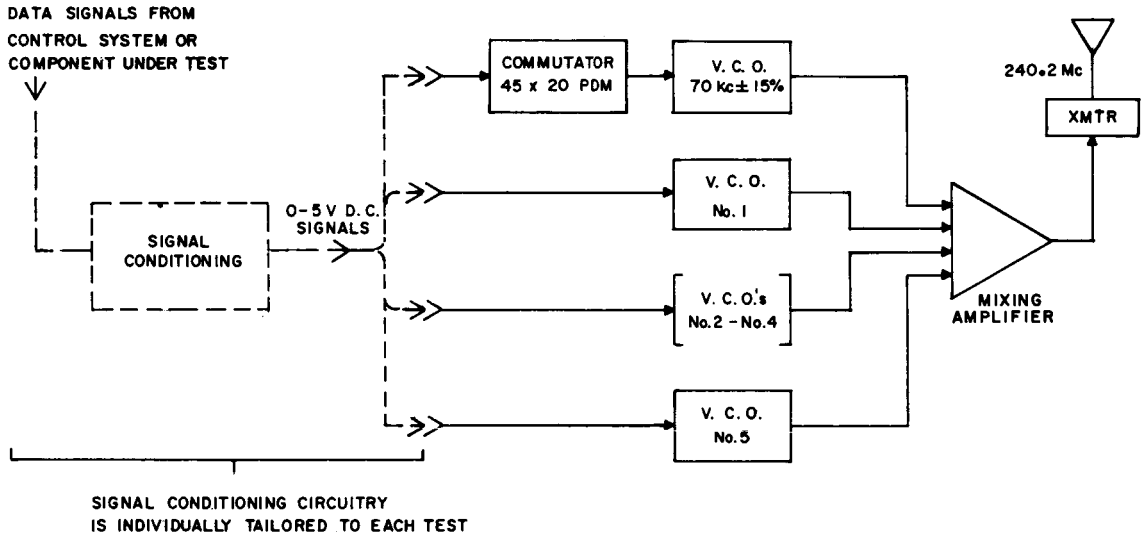

Figure 14. Telemetry Transmission System

IRIG frequencies. Six subcarrier FM channels are used in conjunction with a 45 × 20 PDM commutator. The commutator output modulates a 70 KC subcarrier. The maximum information frequency that can be transmitted via a commutated signal is 2 cps. The other subcarrier channels can transmit information frequencies ranging from 45 cps to 450 cps, depending on the subcarrier frequency. The overall system accuracy in each channel is ±½% of full scale.

The telemetry system is designed to accept standard 0-5V d-c input signals. Hence, signal conditioning circuitry must be designed for any particular test to convert the data signals into 0-5V d-c form.

The mixed output of the subcarrier FM signals is used to modulate an FM transmitter. The carrier frequency of this transmitter is 240.2 Mc with a deviation sensitivity of 100 Kc/volt. The maximum deviation is ±150 Kc with an accuracy of 0.1% for input frequencies between 300 cps and 100 KC. The output of the transmitter is tied to a 50 Ω resistive load in parallel with a 1/8 wave stub

antenna. With this arrangement, the signal strength inside the room is never less than ±1 mv. In the case where the Microthruster table is operated inside a vacuum chamber, the receiving antenna must also be placed inside the chamber. Coaxial cable is then used to bring the radio signal to the ground station.

A single telemetry ground station (see Figure 15) serves both the single axis table and the microthruster table, since it has not proved necessary to

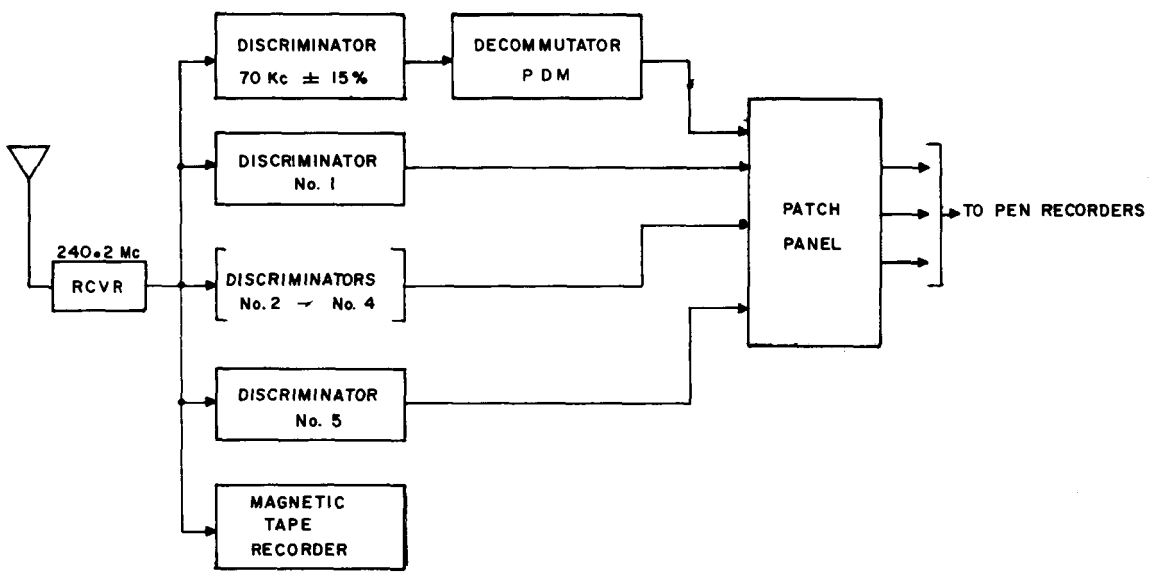

Figure 15. Telemetry Ground Station

operate both tables simultaneously. The ground station consists of an FM receiver, six subcarrier discriminators, and a PDM decommutator.

The output of the FM receiver is fed in parallel to the subcarrier discriminators and the output of the 70 KC discriminator is fed into the decommutator. The multiplexed output of the FM receiver is also fed to a magnetic tape recorder so that data may be recorded and played back at a later time. More important data is recorded in real time on pen recorders. A patch panel in the ground station offers the flexibility of patching any output data signal to any of the pen recorders.

VI. COMMAND SYSTEM

Because of the sensitivity of the single-axis and microthruster tables, it is not possible to send command signals to the table via hard wires, without a serious degradation in table performance. A radio command system was considered, but because of uncertainties in the reliability of transmitting radio frequency signals inside of a vacuum chamber, it was decided to develop a modulated light command system. (This uncertain reliability of radio transmission did not affect the decision to use radio signals for telemetry, since a temporary drop-out of telemetry was not considered critical, whereas a temporary drop-out of command signals could be critical. As it turned out, the radio telemetry transmission was more reliable than expected.) Of course, a light command system requires an unobscured line of sight between transmitter and receiver. This posed no particular problems, even in the vacuum chamber application, since there were numerous glass ports in the sides of the vacuum chamber to be used.

The command system had to be capable of reliably transmitting up to 6 on-off commands, with a time delay of less than 0.1 seconds. Various ways of modulating a light source were considered, among which were frequency modulation and amplitude modulation. To have this system operate over a reasonable distance required the light source to be fairly intense, yet the requirement to modulate this source implied that it has a relatively small thermal time constant. These two requirements to some extent conflict with each other. It was decided therefore that the most practical approach was to use a flashing light and to digitally code the information in the flashes according to their occurrence or non-occurrence. The selected light source was a conventional gas discharge tube which can be reliably pulsed at rates up to about 500 pulses per second, and which yields a fairly intense pulse of light.

All six on-off channels are time multiplexed into one digital word that is transmitted as light flashes along the beam path. The command intelligence is digitally coded in this word and synchronization is accomplished by the absence of light flashes for a prescribed length of time. The system is "fail-safe" in the sense that loss of transmission will turn all channels off. The digital format consists of 32 words per second at a bit rate of 512 per second.

The digital code can be described with reference to Figure 16. If all command channels were off, the digital word transmitted as light pulses would appear as in Figure 16a. These pulses are referred to as the six reference pulses. If a channel is turned on, e.g. channel 3, another pulse will appear one bit time (1/512 sec) after the third reference pulse, as shown in Figure 16b. If

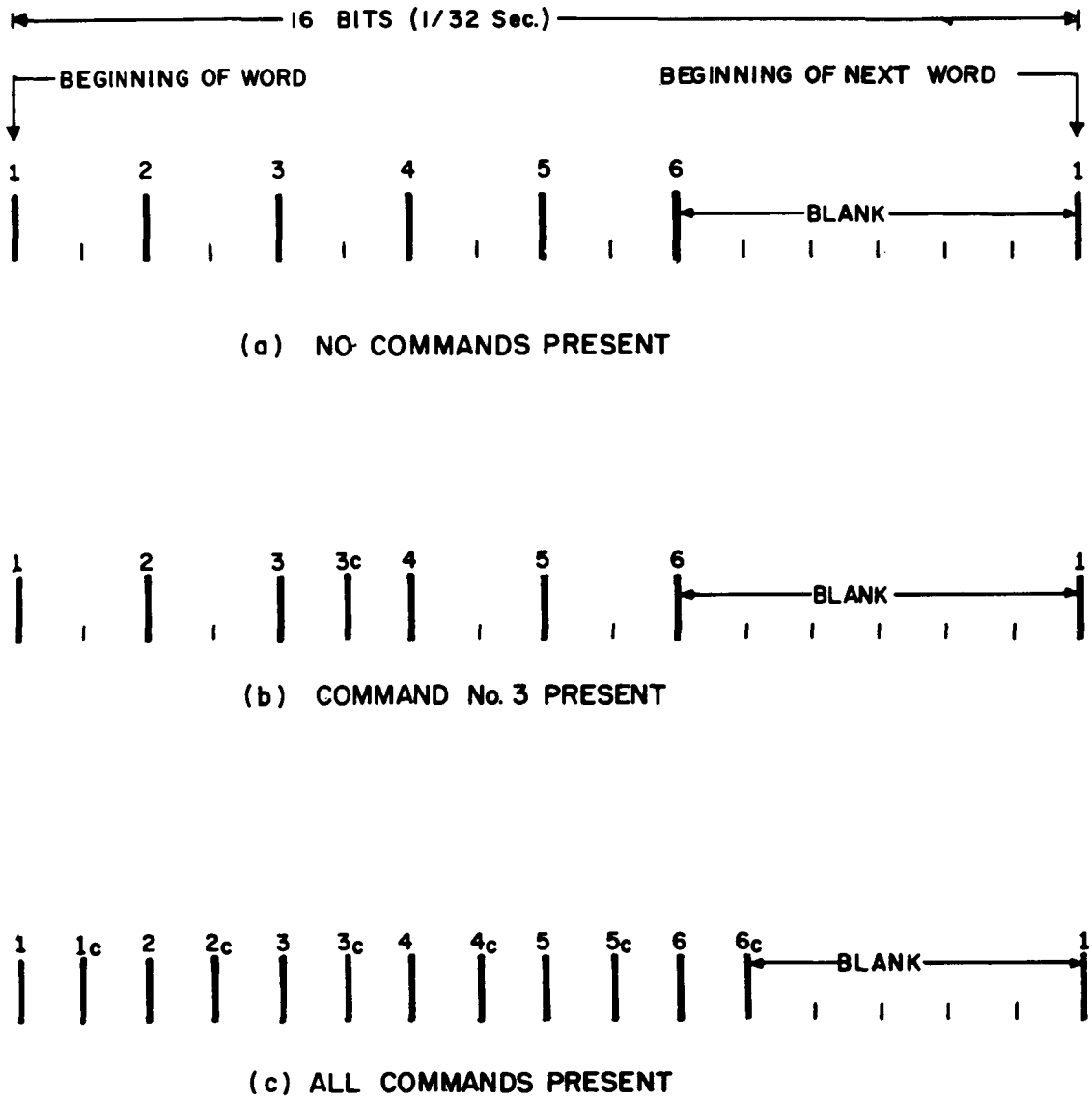

Figure 16. Command System Coding Diagram

all six channels were turned on, the digital word would appear as in Figure 16c.

It will be noticed that regardless of the number of commands transmitted, there is one and only one part of the digital word where there is an absence of 4 or more bits, namely the part following pulse 6 or 6c. This information is utilized by the receiver for word synchronization purposes. The receiver

interprets the next pulse, following the gap of 4 bits or more, as reference pulse 1. This synchronization scheme eliminates the need for a clock in the receiver as well as the need to synchronize such a clock with the one in the transmitter. Thus, the receiver can identify reference pulse 1 and thus all 6 reference pulses in each digital word. It is a relatively simple matter then for the receiver to decide whether the bit following a reference pulse is present or not, and hence whether that particular command is present or not. As a safeguard against an erratic command or command dropout, the receiver circuitry was designed to require the presence of a command pulse in two successive words before turning that command on, and similarly, to require the command pulse to be missing for two successive words before turning the command off. This increases the command response time to 2/32 sec = 1/16 sec, but this was still satisfactory.

The transmitter contains the basic oscillator of 512 cps and the circuitry and logic to fire the gas discharge tube as per the word patterns shown in Figure 16. The particular word pattern transmitted depends on which command switches at the transmitter have been activated. At the receiver a silicon photovoltaic cell serves as the light detector. The received digital word is processed to determine which commands have been activated and the corresponding relays in the receiver are then energized. The details of the transmitter and receiver design are given in Reference 3.

VII. TEST RESULTS — SINGLE AXIS TABLE

The single axis table was tested extensively in both the zero torque and long period oscillation modes. Excellent results were obtained in the zero torque mode. In the long period oscillation mode, the servo system performed as intended, but the test results were masked by the presence of magnetic disturbance torques. This will be discussed later.

Servo tests were run in the zero torque mode to confirm the servo design. Servo velocity following errors were less than 20 arc-seconds for rates up to 1 deg/sec. For a cable with a spring constant of 600×10^{-6} lb-ft/rad (with a 500 lb load the cable spring constant is 845×10^{-6} lb-ft/rad, but decreases with load), the velocity following error represents a torque of only 0.058×10^{-6} ft-lb (0.79 dyne-cm). An open loop frequency response measurement of the zero torque mode indicated a phase margin of 45 degrees. These results were satisfactory.

The major servo system error results from a misalignment between the servo null and the mechanical null, i.e., when the servo is at null (follow-up autocollimator has zero output), the cable may have a small twist resulting in a slight bias torque on the table. In zero torque mode operation, the servo will try to maintain the sensor at null thus maintaining this bias torque. This torque may be reduced by repositioning the autocollimator so that the two nulls coincide. This is accomplished by means of the two micrometer heads associated with the autocollimator mounting plate. For a cable constant of 600×10^{-6} lb-ft/rad, this torque can be reduced to about 4 dyne-cm. Normally, this is done only for operation in the long period oscillation mode, where total disturbance torques must be limited to 10 dyne-cm for proper operation. In the zero torque mode, bias torques up to 100 dyne-cm can usually be tolerated depending on the torque level of the component or system under test. In torque calculations, the measured bias torque is subtracted from the measured total torque.

A typical test utilizing the zero torque mode was the measurement of the momentum associated with a tape recorder for the OAO Spacecraft. The tape recorder, electronics, batteries, and light operated command system were mounted on the table. (The light, 3½ ft diameter, non-magnetic table was used.) The table was oscillated as a torsional pendulum (servo system off) and the period measured. From this data, the total table inertia was determined to be 3.31 slug-ft^2. The system was then put in its operational (zero torque) mode. The bias torques were reduced to about 48 dyne-dm (3.5×10^{-6} lb-ft) which was considered satisfactory for this test.

Two test runs were then made. The first test consisted of putting the recorder in its playback mode via the command system, and allowing it to go through the entire playback cycle of 10.5 minutes. The resultant table position was recorded as a function of time. This data was then graphically differentiated to determine the velocity-time and therefore, momentum profile of the recorder (angular momentum = $J \frac{d\theta}{dt}$ and J is known). The residual momentum at the end of the test (after the tape recorder was shut off) was measured to be 0.00257 lb-ft-sec. This is equivalent to a torque of 4.08×10^{-6} lb-ft acting for 10.5 minutes. This differs from the original measured bias torque by 0.58×10^{-6} lb-ft. Thus the momentum uncertainty at the end of the test was about 0.00037 lb-ft-sec or about 6% of the average recorder momentum of 0.006 lb-ft-sec. The momentum buildup due to the bias torque was assumed linear with time and subtracted from the total momentum to give the recorder momentum profile shown in Figure 17.

In the second test, the recorder was played in one minute increments, as opposed to the continuous run of the first step. Starting with the table at zero velocity the recorder was turned on, allowed to run for one minute, and then turned off. This was repeated ten times to complete the playback cycle. The momentum during each of the increments was determined and plotted in Figure 17. The residual table momentum at the end of each increment was measured and subtracted as in the first test.

As shown in the Figure, the results of the two tests agree very well. The results of the first test are considered more accurate. This is because the residual momentum at the end of each increment of the second test was very small and difficult to measure accurately. All in all, the test results confirmed the capability of the single axis table to measure low torque levels and momentum fairly accurately in the zero torque mode (the estimated accuracy for this particular test, run #1, was about 6%). Greater accuracy can be obtained by taking more time to reduce the servo bias torque level.

Torque disturbances are particularly critical for operation in the long period mode. It can be shown that to achieve a four hour period of oscillation with an inertia of 28 slug-ft^2 (this value of inertia was used in the testing), the unbalance torque on the table must be limited to 0.74×10^{-6} lb-ft (10 dyne-cm). This limit is even lower for longer periods of oscillation. The limit is necessary to keep the servo from saturating when in the long period mode.

Three major sources of torque unbalance have been identified: 1) misalignment between servo and mechanical nulls, 2) air disturbances, and 3) effect of earth's magnetic field. The first source, null misalignment, has been previously

discussed under zero torque mode operation and, as noted there, the effective torque unbalance can be limited to 4 dyne-cm through careful adjustments. The second area, air disturbances, can be critical since a force of only 0.37×10^{-6} lb at the circumference of the four feet diameter table results in the maximum allowable torque disturbance. This problem was alleviated by constructing a reasonably air-tight enclosure around the table to isolate the system from the lab air currents. It is estimated that disturbances due to air currents have been limited to 15 dyne-cm or less. The last source of torque disturbances, magnetic field effects, proved to be the worst, and will be discussed in more detail.

Magnetic torques resulted from the interaction of the earth's magnetic field and some materials on the large capacity, 4 ft diameter table. Although an attempt was made to keep this table non-magnetic, it was not 100% successful. Where strength was important, some parts of the table were made of a 300 series stainless steel. This series is nominally non-magnetic, but still has a permeability of about 1.02. This resulted in interaction with the earth's field to create a torque that is a function of table orientation. This was evident by the fact that in the zero torque mode, the large table had preferred orientations.

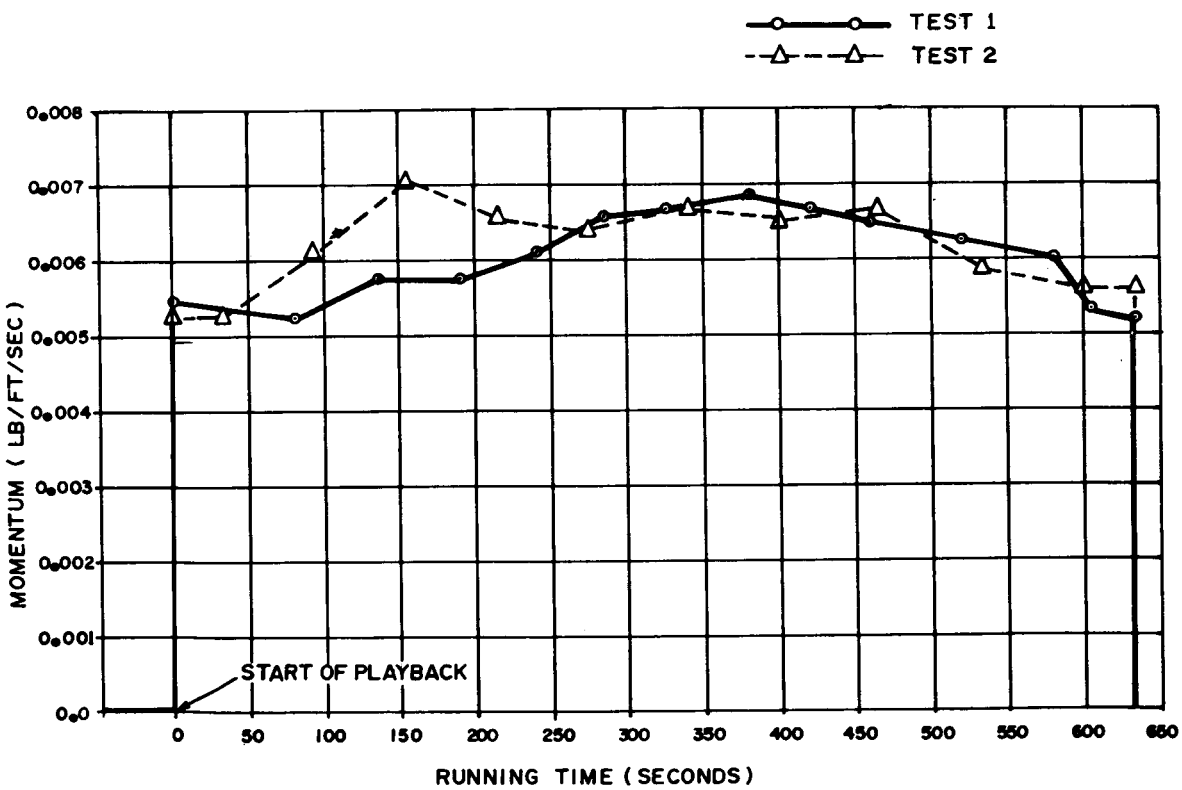

Figure 17. Recorder Momentum Test – Zero Torque Mode

A position sensitive torque is equivalent, for limited angles, to an effective spring constant. When operated in the zero torque mode, and with other disturbances eliminated, the table will oscillate about one of the preferred orientations with a period determined by the inertia and effective magnetic spring constant. Periods of 1½ to 2 hours have been observed. The effective spring constant for this period is much higher than the equivalent spring constant necessary for the long period oscillation mode. Thus these effects will mask any effects of the servo in the long period oscillation mode. This was confirmed by test. When the system was operated in the long period oscillation mode near a magnetic null the softening factor, as indicated by the servo, was near 100. In the absence of all external torques the resultant period should have been close to 4 hours. The period however, was in the 1½ to 2 hour range indicating the predominance of the magnetic torque.

Although the magnetic torque-position profile of the large capacity table is nonlinear and unsymmetric, the estimated peak is less than 11×10^{-6} lb-ft (150 dyne-cm). When this is low compared to the control torque generated on the table, which is true for most control systems, operation of the heavy duty table in the zero torque mode is satisfactory. If not, the smaller capacity non-magnetic table can be used as was the case for the tape recorder test previously described. However, the much smaller inertia associated with the smaller capacity table prevents its use in the long period mode when periods of 4 hours or more are desired.

Even though a 4 hour period was not obtained in the long period oscillation mode, due to the magnetic disturbance torques previously described, the servo system itself performed as expected. This was evident by monitoring the autocollimator output (cable twist) and the feedback pot output and noting that the cable twist was always a stable, small percentage of table motion. This percentage was inversely proportional to the preset softening factor. Thus, it was proved that the system could generate an artificial spring constant that is many times smaller than the natural spring constant of the cable. Of course, in the presence of comparatively large external disturbance torques, this very small artificial spring constant could not achieve the corresponding long period of oscillation.

In order to achieve a 4 hour period with good repeatability, it is estimated that disturbance torques have to be limited to about 5 dyne-cm of steady bias torque and 5 dyne-cm of random disturbance torque. The limit of 5 dyne-cm bias torque can be achieved by the servo system together with a non-magnetic table. The 5 dyne-cm of random disturbance torque can not be achieved outside of a vacuum chamber, since air currents, even inside the enclosure, produce an estimated 15 dyne-cm of random torque. However, the basic system can be

designed to operate inside a vacuum chamber as was demonstrated in the case of the microthruster table, so that there is a high confidence level of being able to achieve "natural" periods of oscillation of 4 hours or longer in the near future. The design of a non-magnetic table system, capable of operating in a vacuum chamber in the long period oscillation mode, will probably await a stronger interest in the testing of gravity gradient dampers or other applications. Meanwhile the present system is being used effectively in the zero torque mode for checkout of control systems and components.

VIII. TEST RESULTS – MICROTHRUSTER TABLE

The Microthruster Table has been tested in both the zero torque and continuous torque modes. Tests have been conducted with a hydrogen diffusion microthruster in a vacuum chamber and with a simple electromagnetic torquer used solely for checking table performance in the continuous torque mode. Though difficulty was experienced with the microthruster, the table itself performed well in all tests.

For microthruster testing, the table has a command receiver, telemetry transmitter, battery power supply, and a removeable microthruster mounting plate as shown in Figure 18. The command and telemetry systems permit commands to be transmitted to the table and various performance data to be telemetered from the table, all without any hard wire links. The battery power supply furnishes power to the telemetry and command components as well as to the microthruster system under test. Removeable microthruster mounting plates facilitate the testing of different microthrusters. The entire microthruster system is mounted on its individual plate, including pneumatics, special electronics, etc., and this sub-assembly is mounted as a unit to the table. A photograph of the completely assembled table inside a vacuum chamber is shown in Figure 19.

The hydrogen microthruster that was tested works on a diffusion principle. The engine is essentially a coiled, dead-end tube of silver palladium that is mounted in a small chamber with a tiny orifice. The tube is connected to a hydrogen supply. The tube can be heated by passing current through it. Heating of the coil causes hydrogen to diffuse through the coil and out through the chamber orifice, thus producing thrust. The hydrogen flow rate, and hence the thrust, is a function of the temperature of the coil as well as the pressure of the hydrogen supply.

A pressure transducer in the small hydrogen tank permitted tank pressure to be telemetered during the test and this data was used for computing flow rate. A temperature transducer at the engine monitored coil temperature. A regulator was used to supply constant pressure hydrogen to the engine. A solenoid valve was added in the line to shut off the flow of hydrogen in case a leak developed in the engine. As it turned out, this solenoid valve permitted the only effective thrust control during the test, because of a small leak in the engine.

The leak in the engine prevented an evaluation of the hydrogen microthruster itself. However, because the leak at any given time was fairly constant, it was possible to measure the thrust produced by this leak and thus evaluate table

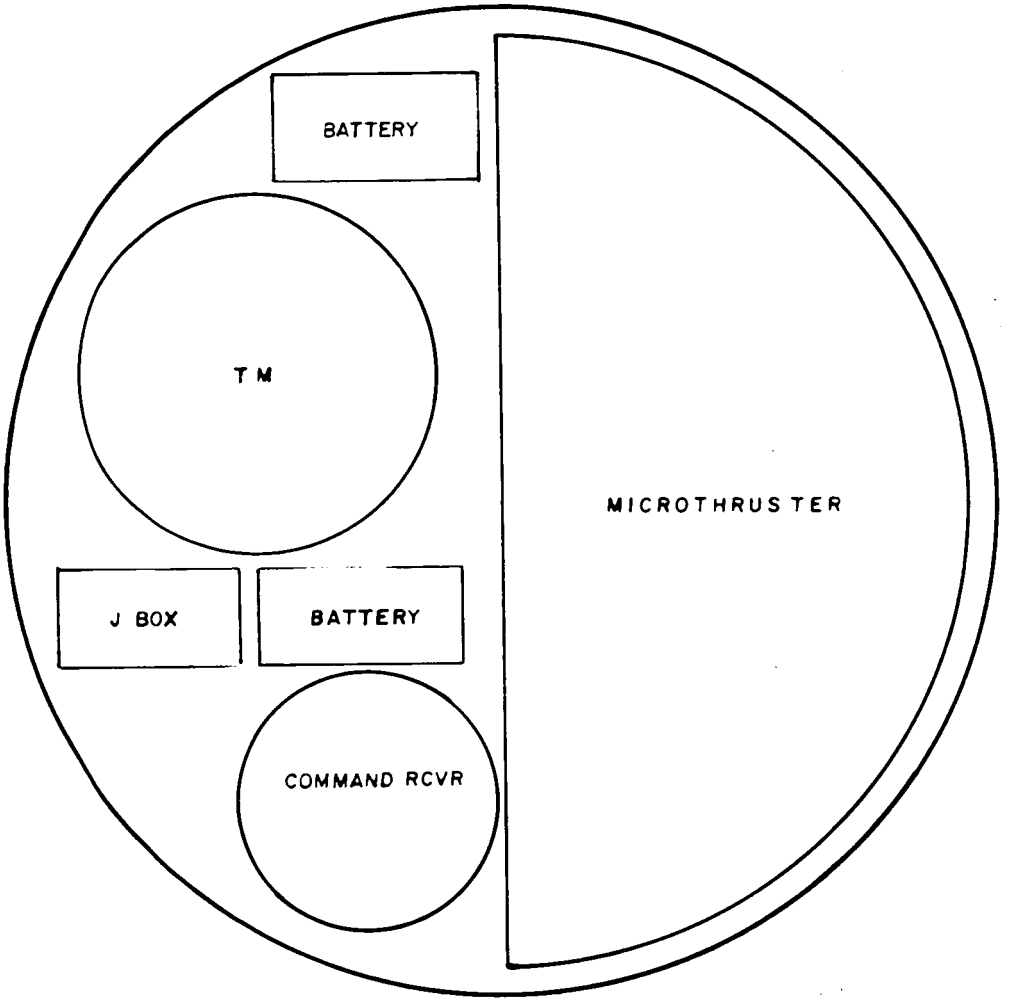

Figure 18. Microthruster Table Layout

performance. The table was run initially in the zero torque mode, and the leak at this time produced a measured torque of 9.78 micropound-ft (132 dyne-cm). A number of runs were made for this condition with good repeatibility. In later tests, the leak had increased to produce a measured torque of 39.2 micropound-ft (530 dyne-cm). Again good repeatibility was obtained over several runs. The table bias torque due to slight misalignment between the servo and mechanical nulls also showed good repeatibility. During one set of runs the bias torque averaged 3.52 micropound-ft and all readings used to give this average were within 0.25 micropound-ft (3.4 dyne-cm). Thus, table performance in the zero torque mode was judged to be good even though the microthruster itself was not functioning properly.

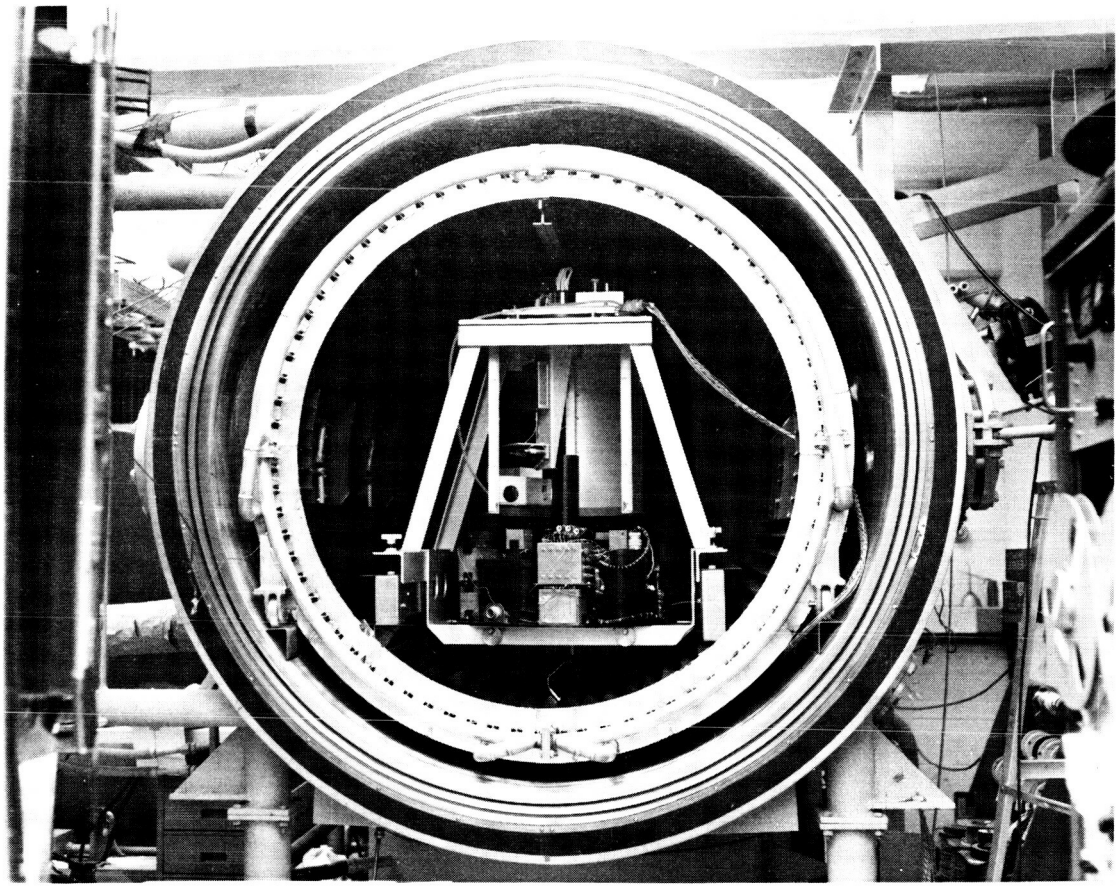

Figure 19. Microthruster Table in Vacuum Chamber

The continuous torque mode was also used for measurement of the torque produced by the microthruster leak. A stiffer cable (K_c = 0.35 dyne-cm/arc-sec) was used in this mode in order to cover the desired torque range of 140 to 1400 dyne-cm (about 10 to 100 micropound-ft).

A number of runs were made with different gain settings of the servoloop. The readings of the fixed autocollimator as well as the follow-up position were used to determine the cable twist and hence torque. Nearly all of the readings during a typical run were within 6 percent of the average (36.2 micropound-ft). Figure 20 (a) shows the output of the fixed sensor in response to the step function torque input (controlled by the solenoid valve). Figure 20 (b) is the corresponding output for the follow-up angle. The response shows good stability with an estimated natural frequency of 0.26 rad/sec.

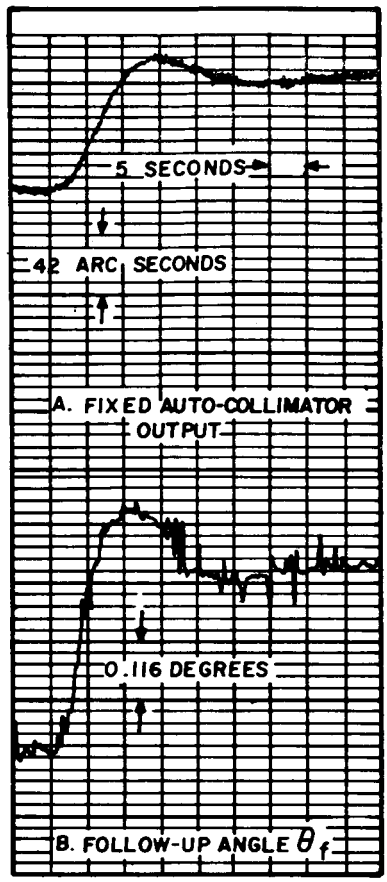

Figure 20. Response of Table in Continuous Torque Mode

Because of the difficulty in obtaining microthrusters with reliable and repeatable characteristics, a simple magnetic torquer was constructed which was used solely for checking table performance in the continuous torque mode. (See Reference 3.) The magnetic torquer consists of an air core coil mounted off the table and a powdered iron amature mounted on the table (see Figure 21). The coil mounting allows the air gap to be preset between 0.5 and 2 inches. (A constant air gap of 1.0 inch was used in the series of tests.) The coil is connected to an adjustable voltage power supply outside the vacuum chamber. The torque is controlled by the amount of current fed to the coil. In the continuous torque mode the motion of the table is negligible compared to the preset air gap, so that the torque is solely a function of the coil current.

The force produced by a solenoid acting on an iron armature through a constant air gap has the general form

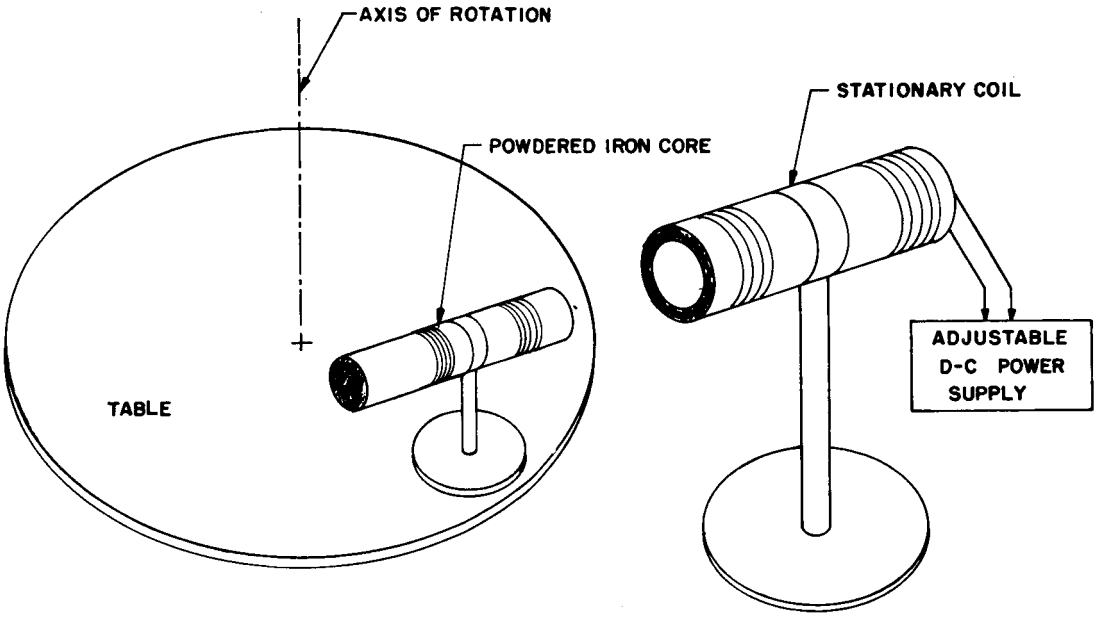

Figure 21. Magnetic Torquer Arrangement

$$F = C_1 NI + C_2 (NI)^2$$

where NI are the ampere turns, C_1 is a constant that depends on the proportions and dimensions of the solenoid and core and on the core material, and C_2 is a constant that depends on the core material and which is inversely proportional to the square of the air gap distance.

Thus, for a limited range of current I, the force or torque produced by the solenoid can be approximated by

$$T = CI^n$$

where n lies between one and two. For large values of current, the quadratic term in F dominates and n would approach two, while for smaller values of current, n would decrease towards one.

The torque produced by the magnetic torquer was measured in the continuous torque mode, using two different cables. The softest cable (K_c = 0.036 dyne-cm/arc-sec) permitted torque measurements from 0.5 to 10 micropound-ft while the

stiffer cable (K_c = 0.36 dyne-cm/arc-sec) permitted torque measurements from 5 to 50 micropound-ft. The saturation of the power supply prevented reaching the top torque of 100 micropound-ft. Where the two ranges overlapped, the measured values of torque were in excellent agreement, which tended to verify the accuracy of the reference spring constants. The measured values of torque over the total range of 0.5 to 50 micropound-ft, as a function of coil current, are plotted on a log-log scale in Figure 22. The smooth curve connecting the measured values is almost a straight line. The slope of this line on the log-log plot is equal to the value of n in the approximate formula $T = CI^n$. It can be seen that n is equal to 2 for large values of current, and decreases to 1.55 at the lowest values of currents used.

The excellent agreement of these measured results with the theory plus the repeatability of the measurements (at least three torque measurements were made at each value of current and nearly all such readings were within 3% of the average) confirm the capability of the table to measure low thrusts accurately.

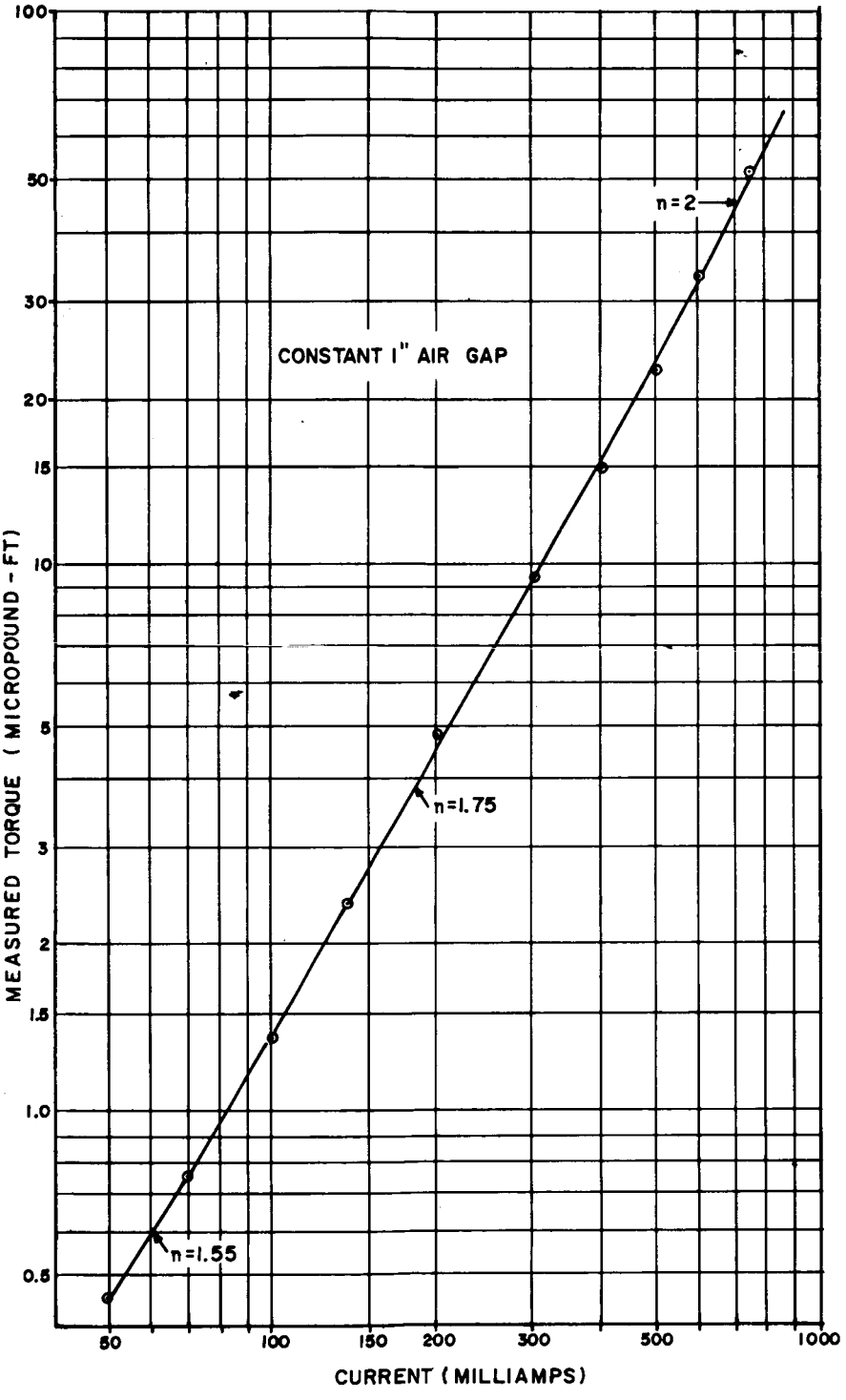

Figure 22. Magnetic Torquer Characteristic

IX. CONCLUSIONS

The basic single axis simulator design, consisting of a soft torsional pendulum with a servo controlled suspension, has proven successful in a variety of applications. In the first model, the single axis table, both a zero torque mode and a long period mode were incorporated. The zero torque mode has provided an essentially zero torque environment for the checkout of control systems and control system components. The servo system can be adjusted to contribute less than 10 dyne-cm of disturbance torque, while external disturbances due to air currents have been limited to about 15 dyne-cm through the use of an enclosure. Disturbance torques due to magnetic effects can be essentially eliminated through the use of a completely non-magnetic table. (This was done on the smaller 3½ ft platform for the single-axis table.) Thus total disturbance torques on the single axis table can be limited to 25 dyne-cm, which is negligible for the great majority of attitude control systems and components.

In the long period oscillation mode, the servo follow-up of the suspensions is controlled in such a way as to maintain cable twist at a small, precise percentage of table motion. This then artificially generates a spring constant that is many times smaller than the already low spring constant of the specially designed cable. In the absence of external disturbance torques, this mode, together with the large inertia table, can generate an extremely smooth oscillation with adjustable periods of 4 hours or more. This would permit the checkout of gravity gradient dampers at the very low rates and frequencies experienced in orbit.

The servo system performed as intended in generating the very small artificial spring constants. Unfortunately, the external disturbances due to random air currents plus the magnetic effects on the heavier table prevented the generation of these very long periods. Magnetic "spring constant" effects dominated to limit periods of oscillation to 1½ - 2 hours. While these effects could be eliminated through a reconstruction of the heavier table, using completely non-magnetic materials, random air currents of about 15 dyne-cm would still hinder effective performance. However, if the system were redesigned to operate in a vacuum chamber, then random disturbances could be limited to a 5 dyne-cm or less. (This was demonstrated on the second model, the microthruster table, which was designed to operate in a vacuum chamber.) Thus, there is every reason to believe that the single axis table can be modified to achieve periods of 4 hours or more in a vacuum chamber. Such redesign will probably await a stronger interest in testing gravity gradient dampers or other applications.

The microthruster table is basically a smaller version of the single axis table, designed for operation in a vacuum chamber. It is able to measure thrusts in the range of one to 200 micropounds, with an estimated accuracy of 8% at the low end and improving to 5% at the high end. It is also able to provide a "zero" torque environment for the single-axis checkout of a complete microthruster control system. For control system checkout the zero torque mode of operation is used. For thrust measurement, either the zero torque mode or continuous torque mode can be used. The latter mode provides continuous, "instantaneous" measurement of torque by utilizing the servo system to turn the suspension so as to continuously counterbalance the torque produced by the thruster with the torque produced by cable twist. This method permits accurate measurement of low level torque with good response and stability. The system natural frequency is about 0.25 rad/sec.

To obtain the same response with a purely mechanical balance would require a much stiffer torsional spring with a consequent reduction in readout accuracy and a severe deterioration in stability because of the absence of damping. Also the stiffer cable would transmit much more vibration, which is a big factor in vacuum chamber operation. The continuous torque mode, with its servo controlled torque balance, either eliminates or greatly reduces these objectionable features.

In summary, the single axis simulator design, with its multi-purpose servo controlled suspension, has proven very successful in the single-axis checkout of attitude control systems and components and in the measurement of thrusts as low as one micropound. It has proven partially successful in the generation of very smooth oscillations of long periods, for checking gravity gradient dampers. A reduction in external disturbance torques, which is feasible under vacuum chamber operation, would in all probability, make this mode operational as well.

X. REFERENCES

1. STL Report 2313-6007-KU000, July 1963, "A Single Axis Space Simulator for Testing the OGO Attitude Control System", by N. H. Beachley.

2. Stabilization & Control Branch Report No. 103, January 6, 1965, "An Ultra-Soft Torsional Cable for a Single-Axis Simulator", by John Hrastar.

3. Stabilization & Control Branch Report No. 154, November 30, 1965, "A Microthrust Test System", by Messr's. Kelly, Cantor, Hrastar, Small and Peterson.